Genome-wide identification and expression analysis of *SBP-box* gene family reveal their involvement in hormone response and abiotic stresses in *Chrysanthemum nankingense*

Ziwei Li[1,*], Yujia Yang[1,*], Bin Chen[1], Bin Xia[1], Hongyao Li[1], Yunwei Zhou[2] and Miao He[1]

[1] College of Landscape Architecture, Northeast Forestry University, Harbin, Heilongjiang, China
[2] College of Horticulture, Jilin Agricultural University, Jilin, China
[*] These authors contributed equally to this work.

ABSTRACT

SQUAMOSA promoter-binding-protein (SBP)-box family proteins are a class of plant-specific transcription factors, and widely regulate the development of floral and leaf morphology in plant growth and involve in environment and hormone signal response. In this study, we isolated and identified 21 non-redundant *SBP-box* genes in *Chrysanthemum nankingense* with bioinformatics analysis. Sequence alignments of 21 CnSBP proteins discovered a highly conserved SBP domain including two zinc finger-like structures and a nuclear localization signal region. According to the amino acid sequence alignments, 67 *SBP-box* genes from *Arabidopsis thaliana*, rice, *Artemisia annua* and *C. nankingense* were clustered into eight groups, and the motif and gene structure analysis also sustained this classification. The gene evolution analysis indicated the *CnSBP* genes experienced a duplication event about 10 million years ago (Mya), and the *CnSBP* and *AtSPL* genes occurred a divergence at 24 Mya. Transcriptome data provided valuable information for tissue-specific expression profiles of the *CnSBPs*, which highly expressed in floral tissues and differentially expressed in leaf, root and stem organs. Quantitative Real-time Polymerase Chain Reaction data showed expression patterns of the *CnSBPs* under exogenous hormone and abiotic stress treatments, separately abscisic acid, salicylic acid, gibberellin A3, methyl jasmonate and ethylene spraying as well as salt and drought stresses, indicating that the candidate *CnSBP* genes showed differentiated spatiotemporal expression patterns in response to hormone and abiotic stresses. Our study provides a systematic genome-wide analysis of the *SBP-box* gene family in *C. nankingense*. In general, it provides a fundamental theoretical basis that *SBP-box* genes may regulate the resistance of stress physiology in chrysanthemum via exogenous hormone pathways.

Subjects Agricultural Science, Bioinformatics, Genomics, Molecular Biology, Plant Science
Keywords *Chrysanthemum nankingense*, *SBP-box* gene, Evolutionary analysis, Expression profile, Hormone response, Abiotic stresses

Submitted 23 May 2022
Accepted 23 September 2022
Published 27 October 2022

Corresponding authors
Yunwei Zhou, dlzhyw@126.com
Miao He, hemiao_xu@126.com

Academic editor
Farrukh Azeem

Additional Information and Declarations can be found on page 24

DOI **10.7717/peerj.14241**

How to cite this article Li Z, Yang Y, Chen B, Xia B, Li H, Zhou Y, He M. 2022. Genome-wide identification and expression analysis of *SBP-box* gene family reveal their involvement in hormone response and abiotic stresses in *Chrysanthemum nankingense*. *PeerJ* **10**:e14241
http://doi.org/10.7717/peerj.14241

INTRODUCTION

Plants may confront a variety of environmental stresses that adversely affect their growth and productivity, such as extreme temperatures, water-deficiencies, drought and salinity stress (*Saibo, Lourenco & Oliveira, 2009*). Plants have evolved many mechanisms to overcome abiotic stresses, including the modification of expression patterns in stress-responsive genes for adaptive development and growth (*Skirycz & Inze, 2010*). Transcription factors (TFs), are groups of important regulatory factors in plants which generally play critical roles in plant growth, differentiation, metabolism mechanism, response to hormone signals and adversity conditions (*Liu et al., 2021b*; *Song et al., 2022*). Plant hormones are the center regulators of physiological reactions and biochemical processes in cells, because they not only initiate internal development perception, but also transmit exoteric environmental inputs. (*Glazebrook, 2005*). The phytohormones, such as abscisic acid (ABA), jasmonic acid (JA), gibberellin (GA), ethylene (ETH), and salicylic acid (SA), integrate environmental stress signaling to mediate the growth and development of plants (*Hou et al., 2013*; *Colebrook et al., 2014*).

SQUAMOSA promoter-binding protein (*SBP*)-box genes encode plant-specific TFs that possess approximately 76 amino acids and a highly conserved DNA-binding domain consisting of approximately 76 amino acid including two typical zinc-finger structures, C3H and C2HC, and a nuclear localization signal region, NLS (*Yamasaki et al., 2004*; *Birkenbihl et al., 2005*; *Guo et al., 2008*). *SBP-box* genes, *AmSBP1* and *AmSBP2*, were initially discovered in snapdragon (*Antirrhinum majus*) due to their interactions with the promoter sequence region of the floral meristem identity gene *SQUAMOSA* (a kind of *MADS-box*), which are relevant to the origin and evolution of reproductive structures such as flowers and ovules (*Klein, Saedler & Huijser, 1996*). In higher plants, the transformation from vegetative stage to reproductive stage of life is an important phase during time of flowering. So it is of great significance to explore the functions of *SBP-box* gene family in chrysanthemum. Since then, *SBP-box* genes have been isolated and characterized in many plants ranging from the single-celled alga (*Chlamydomonas reinhardtii*) (*Kropat et al., 2005*) to model plant, *Arabidopsis thaliana* (*Cardon et al., 1999*) and from world-wide cultivated crops like rice (*Oryza sativa*) (*Xie, Wu & Xiong, 2006*), Chinese cabbage (*Brassica rapa*) (*Cheng et al., 2016*) and wheat (*Triticum aestivum*) (*Li et al., 2020*) to fruits like sweet orange (*Citrus sinensis*) (*Song et al., 2021*), apple (*Malus* ×*domestica* Borkh.) (*Li et al., 2013*) and sugarcane (*Saccharum spontaneum*) (*Feng et al., 2021*).

SBP-box genes regulate many processes of development and floral regulation in flowering plants, including the vegetative phase change (*Xu et al., 2016*), flowering (*Xu et al., 2016*), leaf initiation (*Preston et al., 2016*), shoot and inflorescence branching (*Shao et al., 2019*; *Cui et al., 2020*), fruit development and ripening (Ferreira e (*Silva et al., 2014*)), floral organ development and fertility (*Liu et al., 2017b*) and pollen sac development (*Unte et al., 2003*). It previously reported that *AtSPL3/4/5* redundantly promoted the floral meristem transition and exhibited early-flowering phenotype by binding to the promoters of *LEAFY* (*LFY*), *FRUITFUL* (*FUL*), and *APETALA1* (*AP1*), and acted synergistically with the *FLOWERING LOCUS T* (*FT*)-FD module to induce flowering under long-day (LD)

condition (*Yamaguchi et al., 2009*). In rice, *OsSPL16* participated in the regulation of size, shape and quality of grains (*Wang et al., 2012*; *Yang et al., 2019*) and *OsmiR156k-OsSPL18-DEP1* module regulated the weight and number of grains (*Yuan et al., 2019*).

Previous studies have reported that *SBP-box* genes have a pivotal role in various stresses and hormone signaling pathways (*Wang et al., 2009*). *AtSPL7* and *AtSPL14* separately were pivotal participators in response to copper homeostasis and cell death-inducing fungal toxin fumonisin B1 (FB1) (*Stone et al., 2005*; *Yamasaki et al., 2009*). Over-expression of *AtSPL1* and *AtSPL12* enhanced thermos-tolerance during reproductive growth in inflorescence (*Chao et al., 2017*), and *OsSPL10* negatively regulated salt tolerance in rice (*Lan et al., 2019*). Besides, the *VpSBP* genes in grape overexpressed in *Arabidopsis* improved the tolerance of salt and drought coordinate stress in regulation of salt hypersensitivity (SOS) and reactive oxygen species (ROS) signaling cascades (*Hou et al., 2018*), and *CiSPL* genes in pecan (*Carya illinoinensis*) showed apparent spatiotemporal expression patterns under salt and drought treatments (*Wang et al., 2021*). *VvSBP* and *MdSBP* genes in grape and apple may be dependent on hormonal signaling pathway to reveal involvement in regulation mechanism against abiotic stresses (*Hou et al., 2013*; *Li et al., 2013*) furthermore *PgSPL5* and *PgSPL13* were proved to involve in plant hormone signal transduction in development in pomegranate (*P. granatum*) (*Li et al., 2021*). *CmmiR156*-targeted *CmSBP* genes reduced expression levels via GA signaling pathway in *Castanea mollissima* (*Chen et al., 2019*).

MicroRNAs, miRNAs, a class of endogenous non-coding RNAs, 20–24 nucleotides, were proved to target some *SBP-box* genes and form RNA-induced silencing complexes to regulate functions in plants. In *Arabidopsis* and rice, 11 of 17 and 11 of 19 *SBP-box* genes possessed the *miR156*-targeted sites, which were located in either coding region (CDS) or 3′untranslated region (3′UTR) (*Xie, Wu & Xiong, 2006*; *Xing et al., 2010*). Recently, the involvements of *miR156-SBP/SPL* regulation modules in lots of plant developmental processes and stresses have come to light. *MiR156/529/535-SPL* gene modules regulated the cereal panicle development and higher cytokinin accumulation in female inflorescence in oil palm (*Tregear et al., 2022*). *MiR156* overexpression inhibited non-targeting *SBP* mutation through the raise of DELLA and GA-decomposing enzymes, resulting in stronger phenotypes. And GA also coordinated to other hormones to regulate phase transition *via miR156-SBP/SPL* modules (*Jerome Jeyakumar et al., 2020*). *AthmiR156*-targeted *SPL13* downregulated to enhance the tolerance of drought (*Beveridge & Kyozuka, 2010*). Besides, *miR156*-targeted *SPL2/9/11* genes neutralized negative effects of up-regulated miR156 under heat stress in plant growth and *TcSPLs* in tamarisk showed a critical post-transcription regulation at 1 h under salt stress (*Stief et al., 2014*; *Wang et al., 2019*).

Chrysanthemum is famous for its ornamental and medicinal value regarded as one of the most valuable floricultural crops in the world (*Zhang et al., 2014*). Hybridization and artificial selection extensively exist in genus *Chrysanthemum*, causing that polyploid species and species complexes create highly diversify in ploidy levels, morphology of flowers and leaves, colors of ray florets and environmental tolerances, which bring about great market demand prospects and valuable genetic resources to chrysanthemum breeding (*Ma et al., 2020*; *Qi et al., 2021*). Diversification of growth conditions relatively restrict

the development of the native chrysanthemum resources. Also, soil salinity and moisture increase the production capacity consumption in facility cultivation and become the limiting factor of costs. Therefore, it is significant to investigate the resistance mechanism of chrysanthemum. *C. nankingense* (2n = 2x = 18), a diploid native species of China, processes a key progenitor genomic model (*Yang et al., 2006*; *Ren et al., 2014*). The success of the whole *C. nankingense* genome sequencing is doubtlessly a milestone in the direction of herbaceous plants molecular research, and makes it possible to excavate gene families from genome-wide to provide molecular basis in genetic evolution mechanism (*Song et al., 2018*). It is well known that *SBP-box* gene family acts as a pivotal regulatory in formation of some phenotypes and integration of growth and environmental signals. In tea plant, *CsSBP* genes were response to hormone signals and abiotic stresses, and showed obvious co-expression of *CsSBP2/10* across MeJA, SA and salt treatments (*Teng et al., 2021*). Previous studies mostly focused on flowering mechanism and fruit development, but little known about the potential physiological functions of *SBP-box* family genes. In this study, we performed genome-wide identification of the *SBP-box* gene family in *C. nankingense*, and the characterization, phylogeny, gene structures, *miR156*-targeted genes and tissue-specific expression analysis were investigated by bioinformatics and experiments. We also endeavored to analyze the expression levels of 21 *CnSBP* genes under exogenous hormones and abiotic stresses treatments. This research provided a fundamental theoretical basis of candidate hormone- and stress-responsiveness *CnSBP* genes and further elucidated the potential functions in response to biotic and abiotic stresses dependent on hormone signal pathway.

MATERIALS AND METHODS

Plant materials and treatments

The seeds of *C. nankingense* were preserved with 4 °C in College of Landscape Architecture, Northeast Forestry University (Harbin, Heilongjiang). Lay the soaked seeds flat on a petri dish with wet filter paper at low density, and seeds germinated in two days. The seedlings were cultivated in a growth chamber at a temperature of 25 ± 2 °C with a light/dark cycle of 16/8 h and 60%–70% relative humidity for vegetative growth (*Wang et al., 2022*). At one month of age, the fourth to sixth fully expanded leaves beneath the apex were sprayed with 100 μM salicylic acid (SA), 50 μM methyl jansmonate (MeJA), 100 μM gibberellin A3 (GA_3), 100 mM abscisic acid (ABA) and 0.5 g/L ethylene (ETH) hormone. The roots of seedings were soaked in 200 mmol L^{-1} NaCl and 20% polyethylene glycol (PEG) 6,000 to simulate salty and drought environment. Leaves were sampled followed by 0, 3, 6, 12, 24 and 48 h and immediately stored at −80 °C in preparation for subsequent experiment (*Li et al., 2013*; *Liu et al., 2021a*; *Wang et al., 2021*). The leaf samples of each treatment repeated three times and sprayed with sterile water as the control.

Identification and analysis of *SBP-box* genes in *C. nankingense*

The related genome data of *C. nankingense* was downloaded from chrysanthemum genome database (http://www.amwayabrc.com/zh-cn/index.html), and the BLAST program was set up with local environment for efficient sequence alignments. Protein sequences, coding

sequences and genome data of *Arabidopsis*, rice and *Artemisia annua* were obtained from website (https://www.A.thaliana.org/index.jsp), (https://rapdb.dna.affrc.go.jp/download/irgsp1.html) and NCBI (https://www.ncbi.nlm.nih.gov/genome/). AtSPL and OsSPL protein sequences were used to identify *SBP* gene family members *C. nankingense* with sequence alignments (*E*-value $\leq 1e^{-5}$) in localized BLAST program. Subsequently, NCBI and Pfam (http://www.sanger.ac.uk) were used to search with a hidden Markov model (HMM) profile of the SBP domain (Pfam ID: PF03110) with a cut-off *E*-value of 1×10^{-5} (*Finn et al., 2014*; *El-Gebali et al., 2019*). NCBI-CDD (http://www.ncbi.nlm.nih.gov/structure/cdd/) and SMART (https://smart.embl-heidelberg.de/) were used to confirm whether a complete SBP domain existed or not. InterProScan based on member databases, including CATHGene3D, PANTHER, PROSITE, SUPERFAMILY and InterPro were repeated to search for these proteins in case of the missing or redundancy of SBP domains (*Mulder & Apweiler, 2007*). The selected SBP proteins were renamed CnSBP1-CnSBP21 according to the ascending order of genomic protein IDs. The physicochemical properties of the CnSBP proteins, including relative molecular mass, isoelectric point, average hydrophilic coefficient and others were analyzed by ExPASy (https://web.expasy.org/protparam/) and subcellular localization was predicted by WoLF PSORT (https://www.genscript.com/psort.html). The secondary and tertiary structures of proteins were predicted by SOPMA (https://npsa-prabi.ibcp.fr/cgi-bin/npsa_automat.pl?page=/NPSA/npsa_sopma.html) and SWISS-MODEL (https://swissmodel.expasy.org).

Sequence alignments, phylogenetic and gene structure analysis

Multiple alignments were carried out by DNAMAN 7.0 and ClustalX1.83. Phylogenetic trees were constructed by MEGA 7 software with parameters of neighbor-joining (NJ) method, 1,000 times bootstrap replications and p-distance substitutions model with 50% cut-off partial deletion based on 69 *SBP-box* genes from four species, including monocotyledons (*O. sativa*) and dicotyledons (*Arabidopsis*, *A. annua*, and *C. nankingense*) (*Kumar, Stecher & Tamura, 2016*). The conserved motifs of CnSBP proteins were extracted from MEME website (http://meme.nbcr.net/meme/intro.html) (*Bailey et al., 2006*). The parameters were set as follows: number of motifs: 8; motifs width: 6-50. The conserved sequence logos were obtained through Weblogo (http://weblogo.berkeley.edu) website. The exon-intron structure of *CnSBPs* was extracted by TBtools software according to the genome annotation file (gff.) files (*Chen et al., 2020*).

Calculation of Ka/Ks values

Due to the degeneracy of codons, the difference of paralogous and orthologous gene sequences during species evolution resulted in amino acid change in the encoded protein, which was known as non-synonymous substitution (Ka), conversely, the existence of synonymous codon in same amino acid was called synonymous substitution (Ks). Software DnaSP5 was used to calculate the Ka and Ks values aiming to analyze gene duplication events (*Librado & Rozas, 2009*). The Ka/Ks rate of orthologous and paralogous *SBP-box* gene pairs between *C. nankingense* and *Arabidopsis* was used to determine the selection pressure, and the Ks value can reflect the divergence time during large-scale duplication

events. Divergence time (T) was calculated with the formula T = Ks/2 λ Mya for each gene pair to estimate the date of duplication events. The approximate clock-like synonymous substitution rate (λ) was 1.5×10^{-8} substitutions synonymous/site/year in dicots (*Blanc & Wolfe, 2004*; *Won et al., 2017*).

Promoter *cis*-elements, protein interaction and *miR156*-targeted sites prediction

We extracted 2000 bp sequences from TBtools software as promoters of *CnSBP* genes to excavate *cis*-regulatory elements for further research on regulation mechanism. The *cis*-regulator elements were predicted by PlantCare (http://bioinformatics.psb.ugent.be/webtools/plantcare/html/) website and visualized by TBtools (*Lescot et al., 2002*). STRING (https://string-db.org) online website was used to conduct a preliminary prediction of the homologous proteins of CnSBPs, AtSPLs in *Arabidopsis*, and Cytoscan software was used to visualize the interactive network relationship. We aligned *miRNA* high-throughput sequencing data in *C. indicum* with *Arabidopsis* to obtain *ath-miR156* mature sequences from miRBase (https://www.mirbase.org/) and searched *ath-miR156*-targeted sites in psRNATarget (http://plantgrn.noble.org/v1_psRNATarget) (*Dai, Zhuang & Zhao, 2018*).

Expression profiles of *CnSBP* genes

For increasing insights into potential functions of *CnSBPs*, we analyzed the tissue-specific expression patterns of 21 *CnSBP* genes. RNA-seq data of 6 various plant tissues and organs (leaves (L), stems (S), roots (R), buds (B), ligulate flowers (LF) and tubular flowers (TF)) were downloaded from *C. nankingense* genome database (http://www.amwayabrc.com/zh-cn/download.htm). The expression data was extracted by transcripts per kilobase of exon model per million (TPM) mapped reads using TBtools software. The expression levels of 21 *CnSBPs* were showed by TBtools in the form of heatmaps with parameters of normalized scale method and log scale.

Quantitative real-time PCR analysis

Total RNA was extracted from the frozen samples using Plant RNA Extract Kit R6827 (Omega Bio-Tek, Guangzhou). Single-strand cDNA was synthesized from total RNA using ReverTra Ace® qPCR RT Master Mix (TOYOBO, Japan). Quantitative Real-time PCR was conducted with the UltraSYBR Mixture (Low ROX) (CWBIO, Beijing). The sequences of specific primers were listed in Table S1. All groups of qRT-PCR experiments were performed with three biological duplications, and gene *CmEF1 α* (GenBank Accession No. KF305681) was determined for reference gene (*Zhu et al., 2020*). The relative expression levels were calculated with the $2^{-\Delta\Delta Ct}$ method (*Pfaffl, 2001*).

RESULTS

Identification and characteristics of *SBP-box* family genes in *C. nankingense*

We preliminarily obtained 28 *CnSBP* genes from BLAST sequence alignments and HMMER with a profile Hidden Markov Model (pHMM) of the SBP domain (PF03110). However, seven of them (CHR00008556, CHR00054349, CHR00065414, CHR00077268, CHR00077269, CHR00078717, CHR00084913) were excluded from *SBP-box* family in chrysanthemum for further analysis in SMART and NCBI-CDD database due to their incomplete or redundant SBP domains. Analysis of PfamScan and InterProScan based on different member databases also confirmed complete SBP domains of the filtered CnSBP proteins. Eventually, 21 *CnSBP* genes were determined in *C. nankingense* genome, and we renamed *CnSBP1* to *CnSBP21* based on ascending order of genomic gene IDs.

The amino acid length (aa), relative molecular weight (MW), isoelectric point (PI) and average hydrophilic coefficient (GRAVY) of 21 CnSBP proteins were summarized in Table 1. The amino acid length was ranged from 142 to 954 aa and the molecular weight were in a range of 116447.45–106321.94 Kd. The 21 CnSBP proteins were mostly basic amino acids and unstable proteins, due to the above 7.0 isoelectric point and over 40 the instability coefficient. It indicated that all the CnSBP proteins were hydrophobic due to the negative value of GRAVY except CnSBP14 which was hydrophilic protein. Subcellular localization results showed 19 CnSBP proteins were predictably located in the nucleus but both of CnSBP3 and CnSBP14 were mainly located in endoplasmic reticulum, meaning additional functions may exist in CnSBP3 and CnSBP14. All of 21 CnSBP proteins possessed major secondary and tertiary structures including α-helix, β-helix, random coli and extended strand but the proportion of each structure was distinct (Table S2).

Sequence alignments and phylogenetic analyses

The conserved domain sequences of 21 CnSBP proteins were showed in Table S3. As shown in Fig. 1, 21 CnSBP proteins all have an intact SBP conserved domain (SBP-DBD) which was generally composed of 72-80 amino acid residues. The SBP domain contained three features, the two zinc finger-like structures (Zn1 and Zn2) and a nuclear localization signal region (NLS). CysCysCysHis (C3H) was Zn1 structure for all members except CnSBP14 with another Zn1-like structure CysCysCysCys (C4) which was consistent with AtSPL7 in *Arabidopsis*. While CysCysHisCys (C2HC), the Zn2 structure existed in 18 CnSBP proteins, with the exception of CnSBP2, CnSBP3 and CnSBP12 which lacked part of the C2HC structure. Similar to *Arabidopsis*, the C-terminus of SBP domain in CnSBP proteins owned highly conserved NLS region consisting of a large number of basic amino acid residues. The NLS region shared partial sequence with Zn2 structure and specifically identified GTAC motif that may play an important role in regulating the accurate binding of SBP proteins to target DNA sequence and locating in nucleus (Fig. 1) (*Birkenbihl et al., 2005*; *Riese et al., 2007*).

According to the results, 69 *SBP-box* genes were clustered into eight groups (GI - GVIII) (Fig. 2). The 21 *CnSBPs* were distributed in all eight groups and the largest group (GVIII) contained seven *CnSBPs* accounted for 33.3% of the total *CnSBPs*, whereas GII, GIII, GIV

Table 1 Information on the *SBP-box* family genes in *C. nankingense*.

Gene name	Gene ID[a]	Protein physical and chemical properties				SBP domain location	Homologue of *AtSPL/OsSPL*	Exons	Subcellular localization prediction
		Length[b]	MW (kd)[c]	PI[d]	GRAVY[e]				
CnSBP1	CHR00007823	170	19226.52	9.44	−1.082	59-133	*SPL4/5/OsSPL7*	2	Nuclear
CnSBP2	CHR00009123	163	18557.94	9.08	−0.862	43-110		3	Nuclear
CnSBP3	CHR00009124	258	28789.47	7.47	−0.119	7-74		6	Cytoplasm
CnSBP4	CHR00010885	496	55372.13	6.39	−0.549	110-184	*SPL3/6*	4	Nuclear
CnSBP5	CHR00016731	416	45571.83	6.06	−0.643	140-214	*OsSPL3/12*	4	Nuclear
CnSBP6	CHR00023257	301	33148.32	9.80	−0.590	32-106	*SPL13A/B*	3	Nuclear
CnSBP7	CHR00026823	302	34552.67	8.60	−1.048	195-269	*SPL8*	3	Nuclear
CnSBP8	CHR00027408	954	106321.9	6.16	−0.437	145-219	*SPL1/12/OsSPL6*	11	Nuclear
CnSBP9	CHR00030302	291	32661.65	9.53	−0.738	24-98	*SPL3*	3	Nuclear
CnSBP10	CHR00032503	277	31611.59	9.53	−0.725	38-112	*OsSPL3/12*	3	Nuclear
CnSBP11	CHR00032581	393	43423.35	9.21	−0.664	152-226	*OsSPL3/12*	3	Nuclear
CnSBP12	CHR00053072	233	26179.04	6.13	−0.601	25-99	*SPL13A/B*	3	Nuclear
CnSBP13	CHR00053073	197	22230.78	6.85	−0.779	20-94	*SPL13A/B*	3	Nuclear
CnSBP14	CHR00057355	920	102412.1	6.19	0.018	114-188	*SPL7/OsSPL9*	13	Cytoplasm
CnSBP15	CHR00058779	210	24362.60	9.86	−1.237	127-201	*OsSPL7*	3	Nuclear
CnSBP16	CHR00062917	148	16447.45	9.30	−0.968	57-131	*SPL4/5/OsSPL7*	2	Nuclear
CnSBP17	CHR00063016	310	34975.01	8.87	−0.720	75-149	*SPL3*	3	Nuclear
CnSBP18	CHR00068589	395	43883.86	8.57	−0.770	93-167	*SPL13A/B*	3	Nuclear
CnSBP19	CHR00069886	197	22211.74	6.58	−0.814	20-94	*SPL13A/B*	3	Nuclear
CnSBP20	CHR00075690	428	48515.91	6.93	−0.658	150-203		3	Nuclear
CnSBP21	CHR00083541	142	16626.62	9.28	−1.231	58-132	*OsSPL7*	2	Nuclear

Notes.

[a]Gene ID was corresponded to the annotation provided from *C. nankingense* genome database.

[b]The amino acid length of CnSBP protein.

[c]Molecular weight of CnSBP protein.

[d]Isoelectric point of CnSBP protein.

[e]Grand average of hydropathicity of CnSBP protein.

and GVI contained only one *CnSBP* member. The phylogenetic tree showed that there were 4 groups of paralogous genes in *C.nankingense*, *CnSBP2/CnSBP3*, *CnSBP1/CnSBP16*, *CnSBP12/13/19* and *CnSBP9/CnSBP17*, meanwhile, 10 groups of orthologous genes were found in *Arabidopsis* and *A. annua*. It was worth noting that most *CnSBPs* were highly homologous with *AaSBPs* due to close evolutionary relationships in *Asteraceae* species. Apart from GII, the remaining groups contained *CnSBP* and *AtSPL* gene family members. It was speculated that the *CnSBP* genes have undergone multiple gene replication events from the same ancestral gene and distinct patterns of differentiation occurred among many family members after the separation of each lineage.

Motif composition and gene structures analysis of *CnSBPs*

The typical evolutionary blots and biological functions of TF families were linked with the intron/exon structure, therefore, we analyzed the structural characteristics between 21 *CnSBP* genes and 17 *AtSPL* genes (using the accession number in *Arabidopsis*) (Fig.

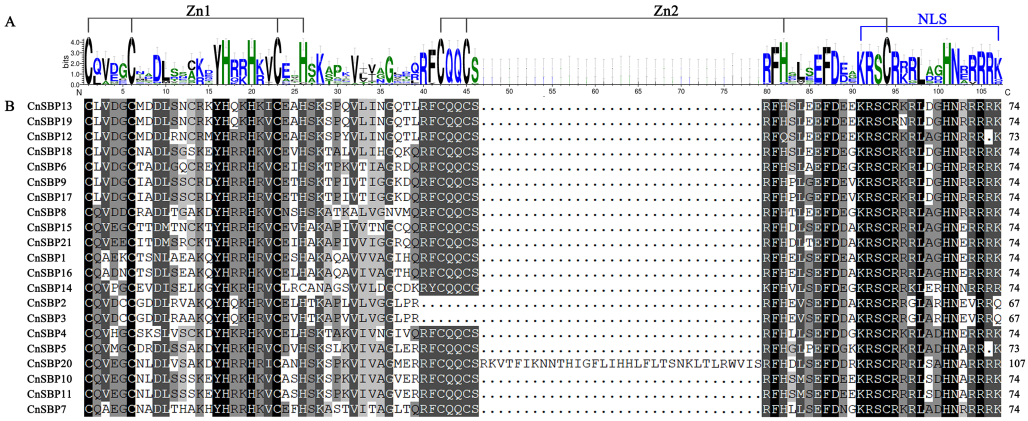

Figure 1 SBP domain alignments of 21 CnSBP proteins. (A) Sequence logo of the SBP domain of CnSBP proteins. The height of the letters within each stack represents the relative frequency of the corresponding amino acids. (B) Multiple alignments of the SBP domain in 21 CnSBPs were performed by DNAMAN 7.0 software. Two zinc-finger structures (Zn1 and Zn2) and a nuclear localization signal region (NLS) were marked.

Full-size DOI: 10.7717/peerj.14241/fig-1

3A). The results revealed that CnSBP8 contained additional gene and motif structures with low complexity sequence repeats regarded as the ankyrin repeat domain (ANK-domain). The protein-protein interaction in ANK-domain mediated diverse and complex biological functions in *CnSBP* genes.

The intron–exon structures indicated that different *CnSBP* genes were diverse, while the same subgroup genes usually possessed similar intron–exon structures, for instance, *CnSBP12*/13/18/19 owned three exons in GVIII (Fig. 2, Fig. 3A). Statistical analyses showed that most *CnSBP* genes contained 2-4 exons, but *CnSBP3*, *CnSBP8* and *CnSBP14* contained 6, 11 and 13, respectively (Fig. 3A). Most members of gene family with shared motifs likely to be an indispensable part to implement important functions or structure compositions. It is particularly critical to excavate new members of gene families by features of conserved motifs. From Fig. 3B, we selected eight motifs within AtSPL and CnSBP proteins and the sequence logos were showed in Fig. S1. It showed that most CnSBP proteins possessed three to six motifs and motif 1, 2 almost simultaneously existed in all CnSBP proteins apart from CnSBP2 and CnSBP3. According to the gene and protein structures, 38 genes were divided into four groups (GA-GD). Members of GD owned two or four extra motifs, which hinted relative specific structures and functions in GD genes. GC members didn't share any other motifs except motif 1 and 2 (Fig. 3B). In order to display the detailed information of the motifs intuitively, the motif 1 and 2 sequence logos were showed in Fig. 3C. On a basis of sequence alignments and domain analysis in above, it was clear that motif 2 corresponded to Zn1 and partial Zn2 finger-like domain, meantime motif 1 contained the complete NLS region (Figs. 3B, 3C). The biological functions of other motifs remained unknown, so it could predicted that some CnSBP proteins had unidentified functions.

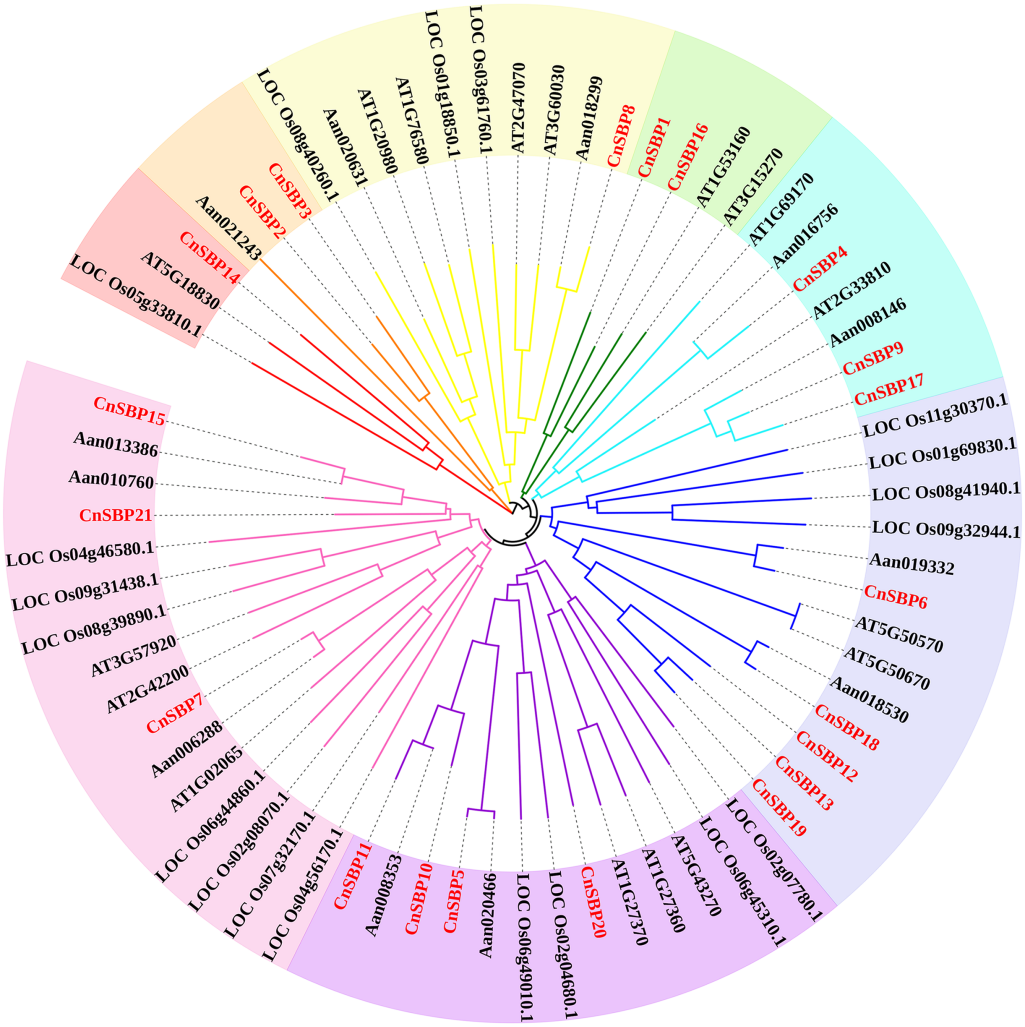

Figure 2 Phylogenetic tree of SBP-box family proteins from chrysanthemum and other species. The neighbor-joining (NJ) method was used to construct phylogenetic tree containing 17 *Arabidopsis* (AtSPL), 19 rice (LOC_OsSPL), 12 *A. annua* (AanSBP) and 21 *C. nankingense* (CnSBP) proteins. The eight sub-groups were colored differently.

Full-size DOI: 10.7717/peerj.14241/fig-2

Gene duplication and evolution analysis of *CnSBPs*

10 paralogous gene pairs (*Cn-Cn*) in *C. nankingense* genome and 6 orthologous gene pairs (*Cn-At*) between the *CnSBP* and *AtSPL* genes were identified with BLASTn and ClustalX. All of the paralogous and orthologous pairs were listed in Table S4. For every homologous gene pair, we calculated Ka, Ks and Ka/Ks values to explore evolutionary selection pressure and investigate the divergence of *CnSBPs* (Table S4). Furthermore, the frequency distributions of the Ks and Ka/Ks values for the homologous gene pairs from *C. nankingense* and *Arabidopsis* were calculated (Fig. 4). The frequency distribution of Ks values for the paralogous pairs in *C. nankingense* averaged ~0.3 (Fig. 4A), indicating that a large-scale duplication event occurred in *SBP-box* gene family in *C. nankingense* approximately 10 million years ago (Mya). Recent research has suggested that the most

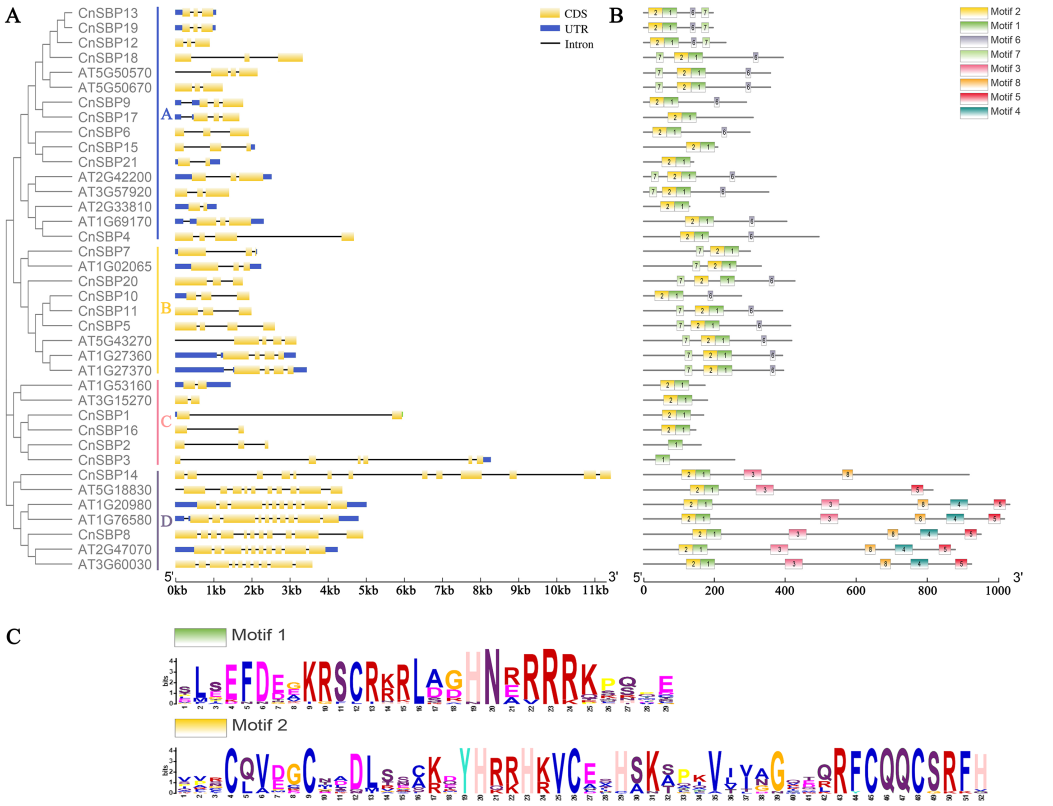

Figure 3 **Phylogenetic tree, gene structures and motif distribution of the *AtSPL* and *CnSBP* genes.** (A) The exon-intron structures of the CnSBPs; exons (CDS) and introns were indicated by yellow boxes and black lines, and blue boxes represented the non-coding regions (UTRs). (B) Conserved motifs of the CnSBP proteins; boxes with different colors and positions represented different structural motifs. (**C**) The sequence logos of motif 1 and motif 2 were visualized by WebLogo online website.

Full-size DOI: 10.7717/peerj.14241/fig-3

recent WGD event in *C. nankingense* occurred ~5.8 Mya, which was a persuasive evidence that the duplicate event of the *SBP-box* genes occurred earlier than whole-genome WGD event. Also, for the *At-Cn* orthologous pairs, the average value at ~0.72 estimated that the divergence time of the *SBP-box* genes was 24 Mya (Fig. 4B). Significantly, the Ka/Ks peaks in the *Cn-Cn* were distributed between 0.5−0.6 (Fig. 4C), while the Ka/Ks in *Cn-At* were 0.7−0.8 (Fig. 4D). On the basis of the values of Ka/Ks, it reflected that the *SBP-box* genes subjected to purification selection (Ka/Ks<1) for homologous gene pairs in *Cn-Cn* as well as *Cn-At*, and tended to eliminate harmful mutations in the population.

Analysis of Cis-regulatory elements in the promoter regions of *CnSBPs*

The distributions and descriptions of critical *cis*-elements corresponding functions of *CnSBP* gene promoters were showed in Fig. 5A and Table S5. Light-responsiveness regulatory elements, including AE-box, 3-AF1, ACE, Box 4, G-box and others were distributed in most *CnSBPs* promoter regions (Fig. 5B). Besides, stress regulatory elements GC-motif, MBS, LTR, ARE, TC-rich and WUN-motif, separately in response to anoxic

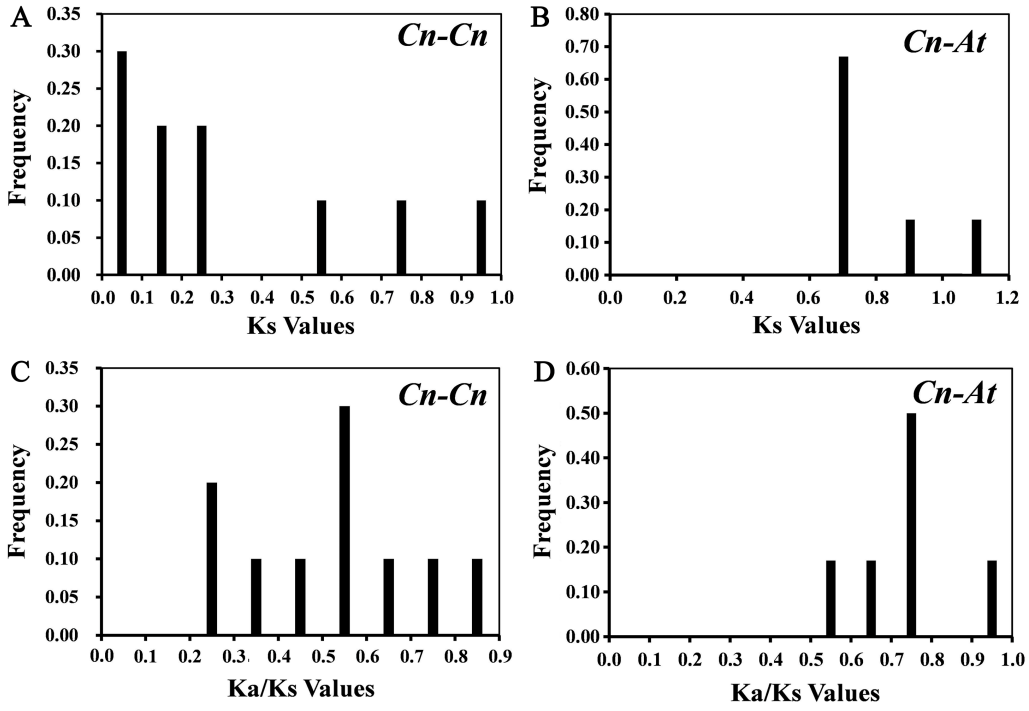

Figure 4 The distribution of the Ks and Ka/Ks values of the paralogous *CnSBP* gene pairs (*Cn-Cn*) and orthologous *CnSBP* and *AtSPL* gene pairs (*Cn-At*). (A, C) Distribution of Ks and Ka/Ks values were obtained from paralogous gene pairs (*Cn-Cn*) in *C. nankingense* genome. (B, D) Distribution of Ks and Ka/Ks values were obtained from orthologous gene pairs (*Cn-At*) between *C. nankingense* and *Arabidopsis* genome.

Full-size DOI: 10.7717/peerj.14241/fig-4

specific inducibility, drought-inducibility, low-temperature responsiveness, anaerobic induction, defense and stress responsiveness and wound responsiveness were respectively identified in 1, 11, 7, 17, 5 and 9 *CnSBP* genes. Likewise, 52 ARE elements occupied the major proportion of stress-responsive elements (Fig. 5B), providing an insight that *CnSBPs* may involve in anaerobic induction.

83 abscisic acid response elements (ABRE), 58 MeJA-responsive elements (CGTCA motif and TGACG-motif), 14 salicylic acid response elements (TCA-element), 10 auxin-responsive elements (TGA-element and AuxRR-core) and 10 gibberellin-responsive elements (GARE-motif, TATC-box, and P-box) were identified (Fig. 5B). The percentage of various hormone-responsive elements were showed in Fig. 5C. It was worth noting that all of the *CnSBP* promoter regions contained at least one hormone-responsive elements. *CnSBP4* and *CnSBP5* only owned ABA-responsive elements and *CnSBP12* owned MeJA-responsive elements (Fig. 5C). Different types and numbers of hormone-responsive elements provided sufficient bases that specific *CnSBP* genes may respond to exogenous hormones and ulteriorly involve in abiotic stresses.

MiR156-targeted sites prediction of *CnSBPs*

Target sites of *miR156* in plants with close relationship tend to conserved in evolution. Due to lack of miRNA sequencing of *C. nankingense*, we used five mature *miR156* family

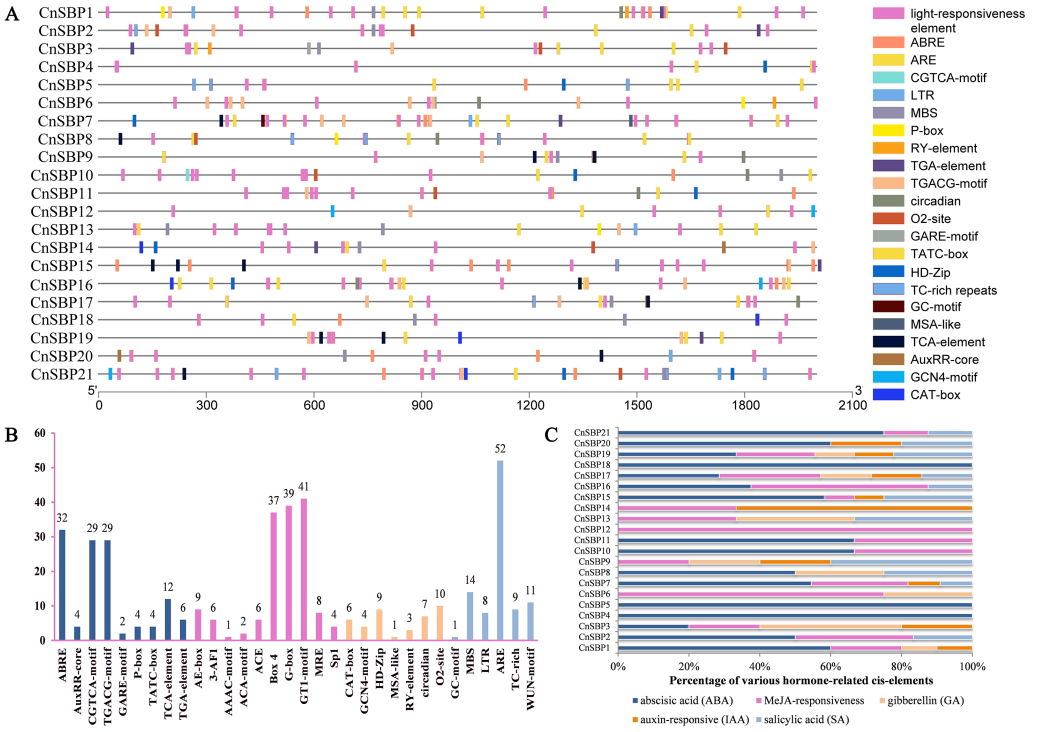

Figure 5 ***Cis*-elements analysis of *CnSBP* genes promoters.** (A) The 2000 bp sequences upstream from the transcription start site were extracted. Different colored boxes represented different *cis*-regulator elements. (B) The total number of *cis*-regulator elements of 21 *CnSBP* genes related to hormone, light, stress and growth responsiveness. (C) Various types of hormone-responsiveness *cis*-elements accounted for the proportion of total hormone-responsiveness *cis*-elements in *CnSBP* genes.

Full-size DOI: 10.7717/peerj.14241/fig-5

members (*Ath-miR156i/j/e/a-5p/f-5p*) in *Arabidopsis* to predict the *miR156*-targeted sites in 21 *CnSBP* genes initially. Multiple sequence alignments of the *CnSBP* genes and reverse complement sequences of *Ath-miR156* showed that 11 *CnSBPs* contained highly consistent sequences with *Ath-miR156* binding sites with no more one to three mismatches (Fig. 6). It suggested that *cna-miR156* may specifically target these genes in *C. nankingense*. These putative *miR156* response elements (MREs) of *CnSBP* genes were located downstream of the *SBP-box* in the coding region of genes in groups GV (*CnSBP4/9/17*), GVI (*CnSBP6/13/18/19*) and GVIII (*CnSBP5/10/11/20*).

Interaction prediction of CnSBP proteins

On the basis of homologous proteins of 21 CnSBP in *Arabidopsis*, it may have functional similarities to further predict the protein functions of CnSBPs. AtSPL proteins in Arabidopsis converged intricate protein-interaction regulation network and SPL5, SPL7 and SPL8 were pivotal central regulators related to complex functions (Fig. 7A). For example, homologous protein of CnSBP1, AtSPL5 converged many interacting proteins, such as SNZ, SMZ, AGL8, AGL20 and TOE2 (Fig. 7B). SNZ and SMZ were AP2-like ethylene-responsive transcription factor and might be involved in the regulation of gene expression by stress factors and by components of stress transduction pathways. It provided

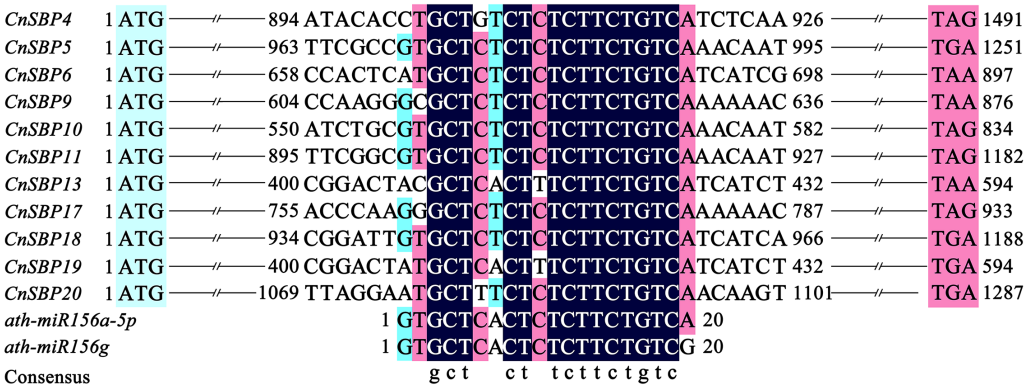

Figure 6 **Alignment of *miR156*-targeted sites complementary sequences within *CnSBP* genes and *ath-miR156* in *C. nankingense* and *Arabidopsis*.**

Full-size DOI: 10.7717/peerj.14241/fig-6

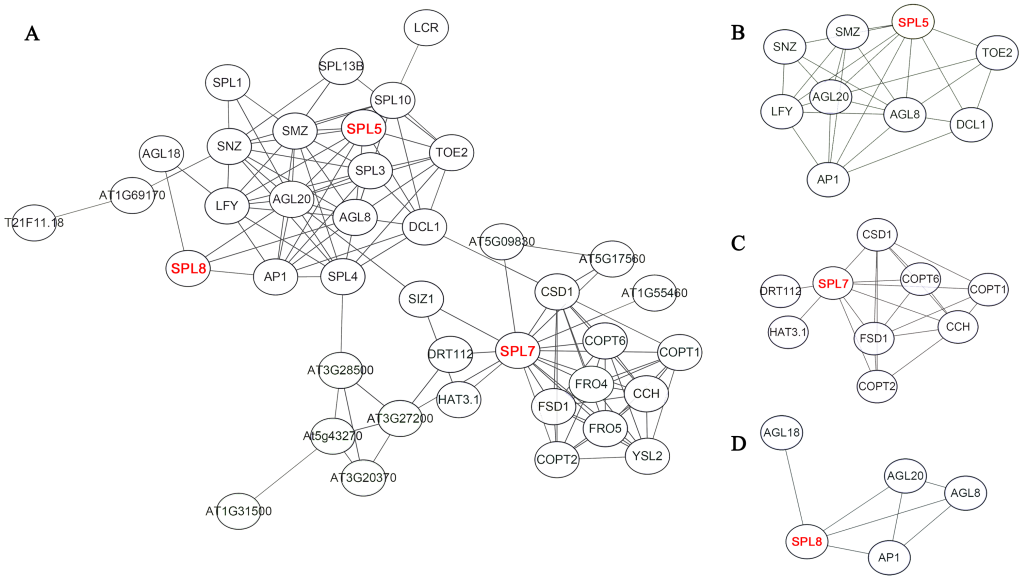

Figure 7 **Potential protein–protein interaction network of CnSBPs.** (A) CnSBP1 and CnSBP16 were clustered with homologous SPL5 protein in *A. thaliana*. (B) CnSBP14 was clustered as homologous SPL7 protein in *A. thaliana*. (C) CnSBP7 was clustered as homologous SPL8 protein in *A. thaliana*.

Full-size DOI: 10.7717/peerj.14241/fig-7

an insight that CnSBP1 might play critical regulation roles in hormone signal transduced pathway and abiotic stresses. AtSPL7 (homologous protein of CnSBP13 and CnSBP20) interacted with SIZ1 which involved in the regulation of plant growth, drought responses, freezing tolerance and salicylic acid (SA) accumulation (Fig. 7C). Besides, SPL8 interacted with AGL8, AGL18, AGL20 and AP1 (*MAD-box* gene family) (Fig. 7D). AGL8 involved in developmental growth in morphogenesis and positively regulated flower development, on the contrary, AGL18 had negatively regulation of flowering. And AGL20 regulated flowering and inflorescence meristem identity and responded to gibberellin.

Tissue-specific expression profiles of *CnSBP* genes

The patterns of gene tissue-specific expression often have a correlation with its encoded protein function. Publicly available transcriptome data of six tissues (root, stem, leaf, bud, ligulate flower and tubular flower) showed transcript levels and cluster analysis (G a-e) of 21 *CnSBP* genes (Fig. 8, File S1). It showed that more than two-thirds of *CnSBP* genes significantly expressed in floral tissues by comparison with one-third expressed in root, stem and leaf tissues. Among these, *CnSBP3* and *CnSBP7* only showed a high expression level in the stage of flower development, and *CnSBP4* evidently expressed in roots. Overall, eight *CnSBP* genes (*CnSBP5/9/11/14/17/18*) in group e shown constitutive expression patterns in all six tissues/organs, while group c and d showed lower expression levels across the nutritive organs than reproduction organs. *CnSBP9*/14/17/18 have relatively high expression levels in leaf and *CnSBP8* and *CnSBP21* significantly expressed in all tissues. With regard to tissue-specific expression patterns, the majority of *miR156*-targeted *CnSBP* genes showed higher expression levels in floral tissues instead of non-targeted *CnSBP* genes. For example, *miR156*-targeted *CnSBP5/9/11/17/18* (members of G e) genes significantly expressed in all tissues, and *miR156*-targeted *CnSBP13/19* genes tended to exhibit higher transcript levels in floral tissues. In terms of *CnSBP* genes in group a, *CnSBP8* expressed ultrahigh transcript levels in all six tissues, and *CnSBP21* similarly showed expression trend but almost no expression in roots (Fig. 8).

Expression profiles of *CnSBP* genes under plant hormone and abiotic stresses

The expression patterns of *CnSBP* genes under plant hormones treatments were examined to the responsive profiles and functions of *CnSBPs* by qRT-PCR (Fig. 9). The raw datas of 21 *CnSBP* genes with ABA, GA, MeJA, SA and ETH treatments were placed in (File S2, S3, S4, S5 and S6). Oligonucleotide primers of 21 *CnSBP* genes and actin gene sequences were listed in Table S1.

Majority of the *CnSBP* genes expression could be induced or inhibited response to GA_3 phytohormones. *CnSBP5*, *CnSBP8*, *CnSBP13* and *CnSBP19* were evidently upregulated by nearly 2.47-, 3.24-, 2.81- and 3.18- fold during 12 h treatment, among these, *CnSBP3/5/13/14/15/19* increased in expression at all stages, but *CnSBP4/8/9* were induced to a peak at 12 h and had a downward trend from 24 h to 48 h (Fig. 9). Under ABA treatment, most *CnSBP* genes downregulated from 3 h to 6 h, but gradually upregulated during the follow-up periods or reached a maximum peak at 12 h. All the remaining *CnSBP* genes displayed a inconspicuous expression fluctuation, for instance, *CnSBP13/14/19* increased after slight drop in expression levels. *CnSBP2/3/7/12* showed an obvious upward trend in response to MeJA before 12 h, *CnSBP4/7/12* performed an obvious decrease in transcript levels from 24 h to 48 h. *CnSBP14/17/18/21* exhibited slightly decreases along with various point of time. Following SA treatment, most *CnSBP* genes presented a decreased trend, except *CnSBP9*/17 prominently increased. Additionally, other *CnSBP* genes displayed slight up- and downregulated fluctuations during processing of SA. Finally, it occurred that the expressions of most *CnSBP* gene upregulated at apex of 12 h or 24 h, but descended from 24 h to 48 h response toETH treatment. In general, *CnSBP1/7/11/14/16/18* significantly

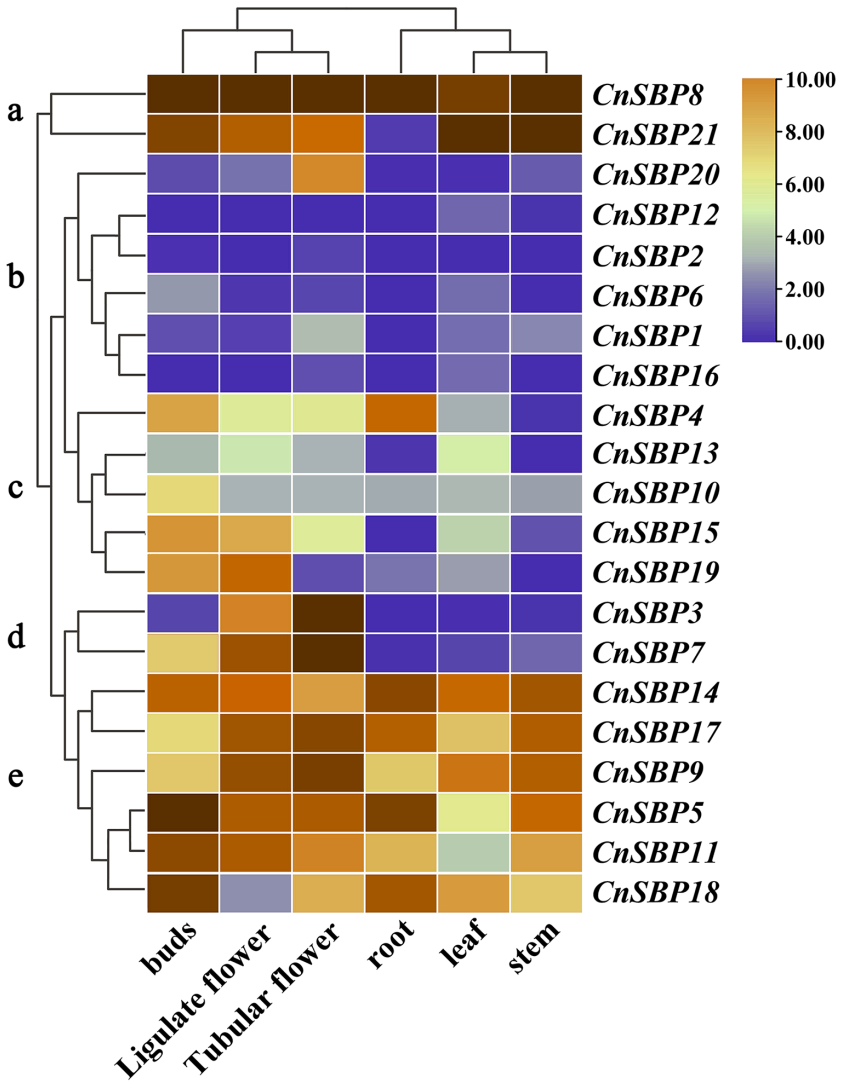

Figure 8 Expression profiles of *CnSBP* genes in six tissues and organs (buds, ligulate flowers, tubular flowers, leaves, roots and stems). Orange and blue indicated high and low expression levels by TPM values in transcript.

Full-size DOI: 10.7717/peerj.14241/fig-8

upregulated during the whole process, and tandem duplicated genes (*CnSBP1/16* and *CnSBP9/17*) showed similar expression pattern throughout various hormone treatments (Fig. 9). We also observed that the same subgroup *CnSBPs* showed a distinct expression trend, such as *CnSBP10, CnSBP11* and *CnSBP20* in GVII (Figs. 2, 9). It suggested that specific *CnSBP* genes might play multiple roles in hormone signal pathway and activate the adaptive regulatory responses in plants and participated in the regulations of abiotic stresses.

In order to investigate the mechanism of resisting stresses dependent on hormone signal pathway, the expression profiles and raw data of 21 *CnSBP* genes in response to salt and drought stresses were examined by qRT-PCR (Fig. 10, File S7 and S8). It

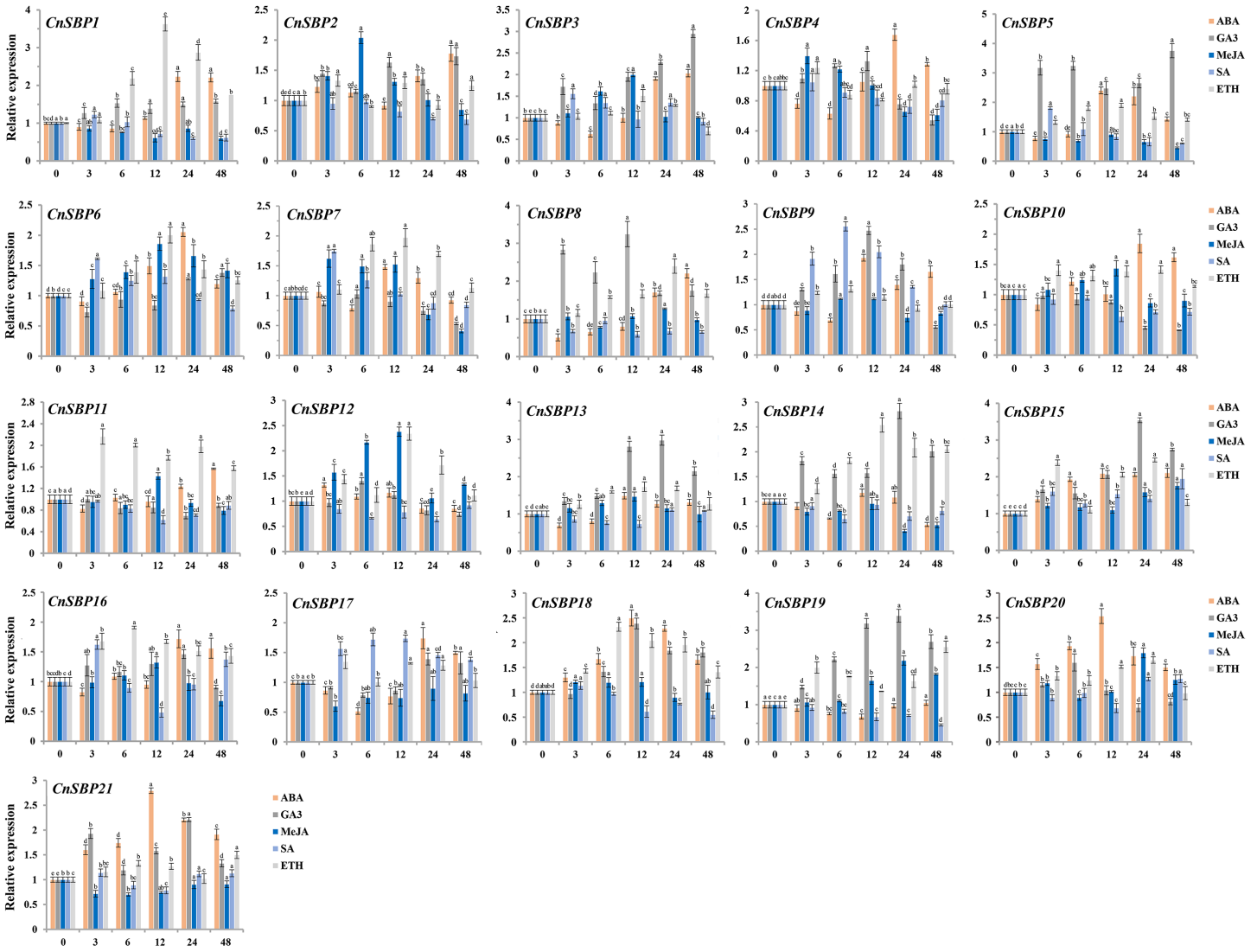

Figure 9 Expression levels of *CnSBP* genes in leaves under hormone treatments by qRT-PCR. The *Y*-axis indicated the relative expression level; *X*-axis (0, 3, 6, 12, 24 and 48 h) indicated hours post hormone treatments. Different colors represented different hormone treatments (ABA, GA3, MeJA, SA and ETH). The standard errors were plotted using vertical lines. The experiments in all panels were repeated three times until convincing results. Bars with different lowercase letters were calculated by one-way ANOVA in SPSS 23.

Full-size DOI: 10.7717/peerj.14241/fig-9

showed that most *CnSBP* genes more or less affected by salt and drought treatments, implying that *CnSBP* genes may play a pivotal role in response to abiotic stresses. In detail, *CnSBP5/12/13* (2.35, 1.50 and 2.05 fold), *CnSBP2/7/20* (2.14, 2.29 and 1.43 fold) and *CnSBP1/3/6/11/15/16/17/21* (1.50, 1.91, 1.63, 1.61, 1.66, 1.62, 1.54 and 2.47 fold compared to 0h) were significantly upregulated by salt stress at early (0 h–6 h), medium (6 h–12 h) and late (12h-48h) responsive periods, respectively (Fig. 10). It exhibited expression trend that firstly increased and then decreased with the passing of time in CnSBP5/7/8/12/13/20. Under drought treatment, *CnSBP12/13/15/18* performed descending expression levels (0.63, 0.47, 0.69 and 0.49 fold at 48 h) during the whole periods of time; *CnSBP7/9//10/14/17/19*

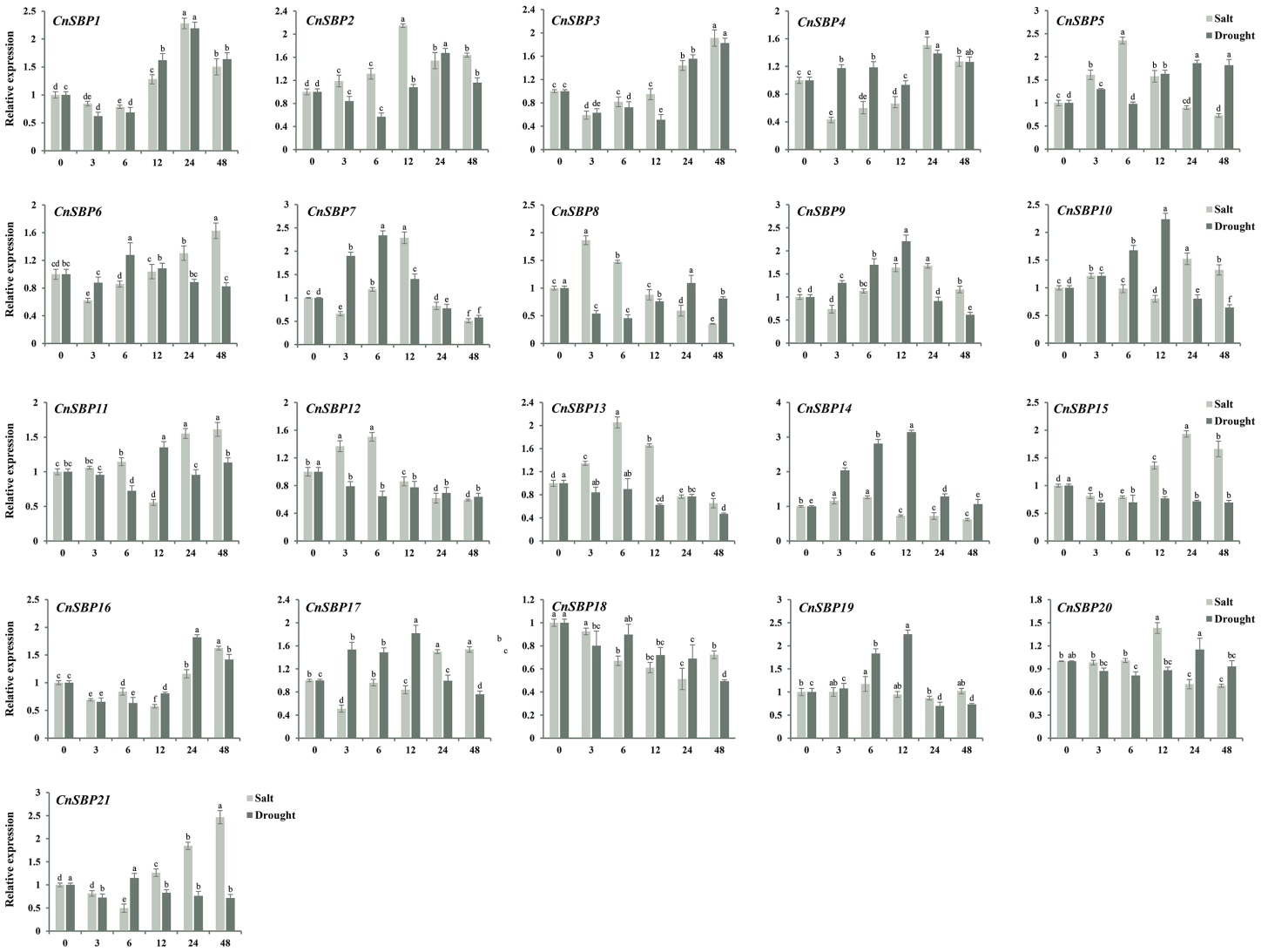

Figure 10 Expression levels of *CnSBP* genes in leaves under abiotic stresses by qRT-PCR. The *Y*-axis indicated the relative expression level; *X*-axis (0, 3, 6, 12, 24 and 48 h) indicated hours post abiotic stresses. Different colors represented different abiotic stresses (salt and drought). The standard errors were plotted using vertical lines. The experiments in all panels were repeated three times until convincing results. Bars with different lowercase letters were calculated by one-way ANOVA in SPSS 23.

Full-size DOI: 10.7717/peerj.14241/fig-10

showed initially increasing then decreasing trend (Fig. 10). Interestingly, the vast majority of *CnSBP* genes had no large multiple differentially induced or downregulated under salt and drought stresses. In general, specific *CnSBP* genes showed co-expression levels in hormone signaling and abiotic stresses, indicating that complex regulatory network covered the processes of plant responsing to stresses and hormone signal transduction.

DISCUSSION

Traditional Chinese flowers, chrysanthemum, is famous for petal colors and floral morphological characteristics. Owning to the nature diploid and progenitor genome, *C.*

nankingense, a close relative of *C. morifolium*, has been considered as a convenient genomic model to research in chrysanthemum (*Song et al., 2018*). Chrysanthemum is susceptible to several abiotic stresses including salt and drought, which has adverse impacts on growth, morphology development, quality, thus leading to serious economic losses. *SBP-box* gene family, a class of plant-specific transcription factor, evolved before the divergence between green algae and the ancestor of land plants, proving that widely involved in life processes such as plant growth, floral development, flowering, fruit ripening, biotic and abiotic stresses and hormone signaling pathway. Identification and expression patterns analysis have discussed on 12 *CmSPL* genes in response to hormones and stresses on the basis of *C. morifolium* transcriptomic data (*Song et al., 2016*). In this study, we identified 21 *CnSBP* family genes from *C. nankingense* genome and provided new insights for comprehensive understanding of the *SBP-box* genes in non-model plants (Fig. 1). Compared with crops, cotton (83 *GhSBPs*), maize (42 *ZmSBPs*), oilseed rape (58 *BnaSBP*) and wheat (50 *TaSBPs*), *C. nankingense* contained much less *SBP-box* genes (*Zhang et al., 2015*; *Cheng et al., 2016*; *Peng et al., 2019*; *Li et al., 2020*), but resembled the model plant *Arabidopsis* (17 *AtSPLs*), flowering plants petunia (21 *PhSPLs*), *Prunus persica* (17 *PpSPLs*), *Prunus mume* (17 *PmSPLs*) and Rosa rugosa (17 *RcSPLs*), indicating that the *SBP-box* family genes endowed with more diversified and complicated functions with species specificity. It could be a consequence of the divergence of flowering responsive functions in *SBP-box* genes.

Physicochemical properties of proteins showed that 21 CnSBP were almost basic amino acids, unstable and hydrophobic proteins. The predictions of secondary and tertiary structures concluded that all CnSBP proteins own similar structures except for subtle diversities, which may lead to various functions (Table S2). Studying the conserved domains of *CnSBP* genes was conducive to highlight the cognition of the *SBP-box* structure. All of the CnSBP proteins contained a complete SBP domain consisting of two zinc finger-like structures (Zn1 and Zn2) and a nuclear localization signal region (NLS) analyzed by Pfam and InterProScan with member databases (Fig. 1). It was unique that the Zn2 and NLS regions shared the common four amino acid residues (KRSC). Unlike other zinc finger structures owned a staggered binding mode, Zn^{2+} and NLS region were necessary for binding to *cis*-elements to the promoters of nuclear genes. Moreover, CnSBP8 possessed an extra ANK- domain in the C-terminal (742-843 aa) of protein, which had a bearing on protein-protein interactions in plant cells (*Lee et al., 2016*). It was clear that the ANK- domain corresponded to motif 4 and motif 8 and encoded correlative exon sequences (Fig. 3). Likewise, CsSBP12 and CsSBP10b in sweet orange and AtSPL14 in *Arabidopsis* with the same ANK- domain were separately in sensitivity to pathogen *Diaporthe citri* and fungal toxin Fumonisin B1 (FB1) (*Stone et al., 2005*; *Song et al., 2021*). It perhaps indicates that *CnSBP8* plays a pivotal role in biotic stresses such as pathogen fungal infection.

Based on phylogenetic tree and gene structure analysis, 21 *CnSBPs* were clustered into eight groups (GI - GVIII) from four species and exhibited closer homology to *Arabidopsis* (17 *AtSPLs*) and *A. annua* (12 *AaSBPs*) rather than rice (*OsSPLs*) suggesting that conservative evolution and common ancestor shared in *Compositae* and dicots plants away from the lineage leading to monocots (Fig. 2). The exon-intron structures and motif analysis also provided significant determinants to cluster phylogenetic tree to a point. The same

group always shared similar structures, such as the members of GVI, CnSBP12/13/18/19 contained motif 1/2/6/7 and three exon distributions (Fig. 3B), indicating that the evolution and gene structures may be interrelated. Besides, separate branch members in GI and GIII owned more complex motifs and gene structures implying that *CnSBP8* and *CnSBP14* may perform additional functions and independent evolution similar to *CsSBP11* in sweet orange (Fig. 3) (*Song et al., 2021*). Intriguingly, on the basis of amino acid sequence alignments, it seemed that CnSBP8 owned a comparable AHA-like domain outside the N-terminal and a IRPGC motif outside the C-terminal of the SBP-domain, which was characteristic of many transcriptional activation domains consistent with CRR1 in *C. reinhardtii* (Fig. S2) (*Riese et al., 2007*). The sequence logos of AHA-like and IRPGC motif were showed in (Fig. S4). The same structures were also found in AtSPLs and OsSPLs clustered with CnSBP8 in group with complex motifs and intron-exon hinting that unknown functions combined with gene structures (Fig. 3, Figs. S2, S3). Furthermore, there was a conserved IRPGC motif existed in downstream of the SBP domain, which was also found in CRR1 in *C. reinhardtii* (Figs. S3, S4) (*Kropat et al., 2005*). It was reported that *SPL7* (homologous gene of *CnSBP8*) played a central role in regulating of Cu^{2+} and transmembrane transporter activity and *SPL12* (homologous gene of *CnSBP14*) regulated root tip and embryonic meristem development, nitrogen metabolism and plant thermos-tolerance at reproductive stage in *Arabidopsis* (*Chao et al., 2017*; *Kastoori Ramamurthy et al., 2018*).

SBP-box genes had underwent duplication event leading to the formation and preservation of multiple paralogs and evolutionary branches. As evident from the phylogenetic tree and BLASTn, 4 pairs of duplicated genes (*CnSBP2/3*, *CnSBP1/16*, *CnSBP9/17* and *CnSBP13/19*) were identified (Fig. 2) in accordance with *Arabidopsis* and rice, indicating that duplicate genes might result in amplified *SBP-box* family in *C. nankingense* (*Yang et al., 2008*). The results of homologous gene comparison for fragment duplication were highly consistent with phylogenetic tree clustering scheme of the evolutionary group (Fig. 2). To explore the macroscopic evolution model in *C. nankingense*, the Ka/Ks ratios for the duplicated gene pairs were estimated. Significantly, the Ka/Ks peak ratios for the *Cn-Cn* and *Cn-At* gene pairs were not difference, respectively, 0.5−0.6 and 0.7−0.8, suggesting that the *CnSBP* genes experienced a strong constraint and purification selection to get adaptive growth in various environment (Fig. 4). As discussed, the Ks values confirmed that the *CnSBP* genes approximately occurred duplication events ∼10 and ∼24 Mya ago earlier than the recent whole genome duplication (WGD) event between *C. nankingense* and *Arabidopsis*, indicating that the *SBP-box* gene family experienced an earlier divergence than the separation of the two most recent species (Fig. 4). In accordance with moso bamboo, *SBP-box* genes family occurred a positive and neutral selection in *CnSBPs* and *PeSPLs* (*Pan et al., 2017*). Additionally, increasing chromosomal localization of *SBP-box* genes in *C. nankingense* may contribute to the deeper understanding of homology and evolutionary relationship.

Remarkably, recent researches found that 11 out of 17 *AtSPL* and 11 out of 19 *OsSPL* genes were targeted by *miR156/157*, here, the miRNA response element (MRE) with speculative *miR156/157*-targeted sites was located downstream of the SBP domain and part of the last exon (Fig. S3) (*Xie, Wu & Xiong, 2006*; *Riese et al., 2007*; *Xing et al., 2010*).

In this study, 11 out of 21 *miR156*-targeted *CnSBP* genes were calculated and all clustered in clades of GV, GVI and GVII with common conserved region in motif 6 (Figs. 2, 3B). It was consistent with previous researches that proved 11, 6, 12 and 19 *miR156*-targeted *SBP-box* genes in *P. mume*, melons, grape and walnut. It may be a major determinant of *miR156*-targeted *SBP-box* genes to carry out distinctive and significant functions with *miRNA-SBP/SPLs* modules in evolution. The *miR156b* targeted two paralogous genes, *SPL9* and *SPL15*, controlled shoot maturation and the temporal initiation of rosette leaves (*Schwarz et al., 2008*). TaSPL3/17 interacted with DWARF53 to reveal potential association in SL signaling pathways during bread wheat tiller and spikelet development by *miR156* targeted *SPL* genes (*Liu et al., 2017a*). Besides, *miR156*-targeted *CnSBP5/10/11/13/17/18/19* highly expressed in floral organ (Fig. 7), demonstrating that *CnSBP* genes, as well as their regulators *miR156* remained to regulate flower morphological characteristics. It would be relevant that *SPL3* (clustered with *CnSBP9* and *CnSBP17*) regulated by *miR156* to integrate endogenous signals into flowering pathway (*Gandikota et al., 2007*).

Protein-interaction network conducted a preliminary prediction of CnSBP proteins. Through interacted relationships, it provided insights that CnSBP5 might play a critical regulation role in hormone signal pathway and abiotic stresses. And the homologous protein of CnSBP7, AtSPL8, largely involved in promoting flowering, inflorescence meristem identity and GA response. In summary, CnSBP proteins may combine with correlative genes involved in biotic and abiotic stresses, phytohormone pathway as well as growth and development in plants.

Tissue-specific expression analysis showed that most *CnSBP* genes highly expressed in floral organs possibly due that SBP proteins interacted with the *SQUAMOSA* (a *MADS-box*) promoter, a floral meristem gene correlated with the origin and evolution of reproductive organs such as flowers and ovules. Eight members (*CnSBP5/8/9/11/14/17/21*) showed high levels expression in all tissues regarded as significant regulatory factors in plant growth process (Fig. 8). In group b, six *CnSBP* genes exhibited lower expression levels in six tissues compared with other members. Interestingly, paralogous genes *CnSBP2* and *CnSBP3*, differentially performed expression levels in floral organs, it perhaps associated that the expanded *CnSBP* genes occurred functional divergence resulting in novel biological functions. In group c, same subgroup members *CnSBP13* and *CnSBP19* expressed in floral organs and leaves. Likely, homologous gene *AtSPL13A/B* participated in the formation of leaf shape and reproductive stages. Furthermore, *AtSPL3* (clustered with *CnSBP4*) regulated flowering time and activated downstream gene expression during flowering morphological development (*Jung et al., 2012*). *OsSPL9* (clustered with *CnSBP14*) regulated the number and yield of grains as well as Cu accumulation and metabolism in rice, suggesting potential roles in *CnSBP14* (*Tang et al., 2016*).

During the lengthy evolution of organisms, plants have obtained complex genic regulatory mechanisms to mitigate effects from adverse environments. Both enzymes and hormones were crucial means by which plant affected a series of physiological or biochemical changes to gain adaptive capacity to resist the stresses (*Sah, Reddy & Li, 2016*). In the study, a further finding was that numerous of hormone-responsive elements as well as stress-responsive elements were exhibited in *CnSBP* promoters, hinting that 21

CnSBP genes may have an intense response to hormone signal and abiotic stresses (Fig. 5). Therefore, in line with the ideas that co-expression of genes in response to abiotic stresses and exogenous induction were considered as candidate genes to involve in regulation. Consequently, we researched the expression profiles of the *CnSBP* genes under ABA, SA, MeJA, GA_3 and Eth hormone treatments. Exogenous spraying induction can not only activate the expression of defense-related genes, but also interconnect hormonal signal network with defense responses. Expression analyses showed that 11 out of 21 members were significantly induced by ABA treatment at 12 h with a high proportion of ABA-responsive elements (Figs. 5, 9). ABA, regarded as a positive signal of stress, can improve plant tolerance to variable environment by inducing the production of H_2O_2 and establish ROS balance (*Mittler & Blumwald, 2015*). Research showed *OsSPL7* (orthologous gene of *CnSBP15* and *CnSBP21*) in rice was proved to play a critical role in ROS balance in response to biotic and abiotic stresses (*Hoang et al., 2019*), indicating that *CnSBP15* and *CnSBP21* may involve in stress responses *via* ABA signaling pathway. In our study, *CnSBP15* and *CnSBP21* significantly induced by ABA and salt treatments. 10 out of 21 members were markedly induced by GA_3 treatment with poly-type GA-responsive elements, which may represent more complex expression and regulation patterns (Fig. 5, Fig. 9). An example was *AtSPL3*, clustered with *CnSBP4*, integrated photoperiod and GA signals to regulate flowering *via* SOC1-SPL module (*Jung et al., 2012*). In chinese chestnut, *CmSPL6/CmSPL9/CmSPL16* highly and *CmmiR156* lowly expressed during flowering development by exogenous GA_3 spraying (*Chen et al., 2019*). Moreover, we revealed *CnSBP6/9/17* prominently induced by SA and salt treatments at 24 h and 48 h time points, and *CnSBP6/7/12* induced by MeJA but downregulated by drought treatment at 48 h time point (Fig. 9). It confirmed that plants induced trans-activating factors to activate promoters of defense genes related to SA pathway to improve resistance in *Arabidopsis* (*Dong, 1998*). In grape, *VvSBP17* was upregulated response to SA and pathogen infection treatment which was the same as homologous gene, *AtSPL14*, in sensitivity to fumonisin B1 (FB1) (*Hou et al., 2013*). Previous studies have proved *miR156*-resistant *SPL13* involved in ethylene biosynthesis by upregulating the expression of *ACC* oxidase gene in accordance with the same subgroup members, *CnSBP12/13/18/19*, with inductive expression patterns. Similarly, 12 *MdSPLs* upregulated and one *MdSPL* downregulated in apple by exogenous ethylene spraying (*Li et al., 2013*). Bioinformatics and molecular technology were limit to explore complex functions of *SBP-box* genes, subsequently the physiological biochemistry of candidate *SBP-box* genes need to investigate in future studies to better clarify regulatory network of various environment conditions.

Although the dominant roles of *SBP-box* genes have been explored in processes of plant growth and development, the cross-talk analysis between various stresses and hormonal response were also worthy to discuss. SA and MeJA can active multiple defense strategies and converge complex signaling networks to enhance the stress resistance capacity in plants, such as salinity stress (*Qiu et al., 2014*; *Kim et al., 2018*). In grape, the expression of *VvSBP9/14/16* were downregulated expression in response to SA and MeJA and salt stress (*Hou et al., 2013*). *CsSBP3/4/8/13* genes in tea plant (*Camellia sinensis*) significantly upregulated under MeJA and drought treatments (*Zhang et al., 2020*). DELLAs and some

regulators in GA and ABA signaling pathway participate in the regulation of tolerance in response to abiotic stresses in plants. Special *PeSPL* genes induced by GA but inhibited by drought stress in moso bamboo (*Pan et al., 2017*).

In our study, most *CnSBP* genes exhibited various transcript levels but presence of co-expression candidate genes confirmed that *SBP-box* family regulated the resistance physiology of chrysanthemum *via* by complex stress responsive mechanism and regulation network. qRT-PCR analysis showed *CnSBP1/3/5/16* were upregulated and *CnSBP8/12/13/15/18* were downregulated under drought stress (Fig. 10). Among these, most *CnSBP* genes were prominently induced by at least one hormone accompanied by MBS (drought-inducibility) *cis*-elements in promoter regions. The expression levels of *CnSBP1/3/9/13/15/18/21* were significant under salt treatment perhaps because they integrated with TC-rich repeats in promoter regions (Fig. 5, Fig. 10), which was regarded as defense and stress responsiveness *cis*-element. In rice, overexpression *OsSPL10* (clustered with *CnSBP7* and *AtSPL8*) weakened salt tolerance (*Lan et al., 2019*). In Alfalfa, *MsamiR156-MsSPL* module partially improved drought tolerance *via* overexpression *MsamiR156* to silence *MsSPL13* (*Arshad et al., 2017*).

In addition, lots of evidence indicated that *miR156/SBP* (*SPL*) modules regulated a variety of developmental processes and abiotic stress response in plants (*Jerome Jeyakumar et al., 2020*), for instance, the upgregulated expression levels of *ath-miR156* inhibited targeted *SPL2/9/11* genes to balance the adverse bearing on heat stress during plant growth and development (*Stief et al., 2014*). Besides, it was reported that *MdWRKY100* gene expression was upregulated by *miR156/SPL* module to regulate salt tolerance in apple (*Ma et al., 2021*). Recently, genetic engineering means aim at enhancing tolerance of abiotic stresses by modifying *miR156*-targeted nodes and elucidating targeted genes will expand adaptive plants to abiotic stresses. With sequence alignments of *miR156*-targeted genes sites, it preliminarily cleared that specific *CnSBP* genes were core factors in integration of phytohormone signaling and abiotic stresses, which need to verify by further experiments in future.

CONCLUSIONS

In this study, we identified 21 *SBP-box* genes in *C. nankingense* genome and provided a comprehensive overview of SBP transcription factor family in chrysanthemum. 21 *CnSBPs* were classified into eight groups based on *SBPs* (*SPLs*) genes in *Arabidopsis*, rice and *A. annua* and closer homology with *Arabidopsis* and *A. annua*. Further analysis of conserved domain, motifs, gene structures, gene duplication and evolutionary supported classification results. Subsequently, we predicted physiochemical properties, secondary and tertiary structures, promoter *cis*-regulator elements, *miR156*-targeted sites and protein-protein interaction of 21 *CnSBP* genes. Tissue-specific expression profiles revealed that *CnSBPs* may play a pivotal role in floral organ growth and development. *CnSBPs* also responded to exogenous hormone induction and abiotic stresses. The expression patterns with same clustering results tended to be consistent. Taken together, our results helped shed light on *SBP-box* gene basic information in *C. nankingense* and provided an experimental

basis on the functions of *CnSBP* genes in plant growth regulation. Candidate *CnSBP* genes should further elaborate comprehensive understanding of the co-related regulatory patterns of hormone responses and abiotic stresses. It laid a theoretical foundation for the subsequent study of *miR156/SBP* (*SPL*) modules regulation mechanism and improvement of chrysanthemum breeding.

ACKNOWLEDGEMENTS

Special thanks to Dr. Fadi Chen and Dr. Shilin Chen of Nanjing Agricultural University and Institute of Chinese Materia Medica for the provision of *Chrysanthemum nankingense* genome and transcriptome data used in this study. We are grateful to Dr. Nuananong Purente for her help in English proofreading. We would like to thank Dr. Farrukh Azeem Editor and three reviewers for their professional and helpful comments on the original manuscript.

ADDITIONAL INFORMATION AND DECLARATIONS

Funding

This research was supported by the National Key Research and Development Program of China (2018YFD1000406), the National Key Research and Development Program of China (2019YFD1001504) and the Natural Science Foundation of Heilongjiang Province, China (No. LH2021C018). The funders had no role in study design, data collection and analysis, decision to publish, or preparation of the manuscript.

Grant Disclosures

The following grant information was disclosed by the authors:
The National Key Research and Development Program of China: 2018YFD1000406.
The National Key Research and Development Program of China: 2019YFD1001504.
The Natural Science Foundation of Heilongjiang Province, China: LH2021C018.

Competing Interests

The authors declare there are no competing interests.

Author Contributions

- Ziwei Li conceived and designed the experiments, performed the experiments, prepared figures and/or tables, authored or reviewed drafts of the article, and approved the final draft.
- Yujia Yang performed the experiments, prepared figures and/or tables, and approved the final draft.
- Bin Chen analyzed the data, authored or reviewed drafts of the article, and approved the final draft.
- Bin Xia analyzed the data, authored or reviewed drafts of the article, and approved the final draft.
- Hongyao Li analyzed the data, prepared figures and/or tables, and approved the final draft.

- Yunwei Zhou conceived and designed the experiments, authored or reviewed drafts of the article, and approved the final draft.
- Miao He conceived and designed the experiments, authored or reviewed drafts of the article, and approved the final draft.

DNA Deposition

The following information was supplied regarding the deposition of DNA sequences:

The reference gene, CmEF1α, sequences described here are available at GenBank: KF305681.

Data Availability

The following information was supplied regarding data availability:

The raw data are available in the Supplemental Files.

The raw data for ABA, GA, SA, MeJA, ETH, salt and drought treatments of CnSBPs is showing the involvement of the SBP-box gene family response to hormone response and abiotic stresses in Chrysanthemum as well as the transcript expression levels in different tissues.

Supplemental Information

Supplemental information for this article can be found online at http://dx.doi.org/10.7717/peerj.14241#supplemental-information.

REFERENCES

Arshad M, Feyissa BA, Amyot L, Aung B, Hannoufa A. 2017. MicroRNA156 improves drought stress tolerance in alfalfa (*Medicago sativa*) by silencing *SPL13*. *Plant Science* **258**:122–136 DOI 10.1016/j.plantsci.2017.01.018.

Bailey TL, Williams N, Misleh C, Li WW. 2006. MEME: discovering and analyzing DNA and protein sequence motifs. *Nucleic Acids Research* **34**:W369–W373 DOI 10.1093/nar/gkl198.

Beveridge CA, Kyozuka J. 2010. New genes in the strigolactone-related shoot branching pathway. *Current Opinion in Plant Biology* **13**:34–39 DOI 10.1016/j.pbi.2009.10.003.

Birkenbihl RP, Jach G, Saedler H, Huijser P. 2005. Functional dissection of the plant-specific SBP-domain: overlap of the DNA-binding and nuclear localization domains. *Journal of Molecular Biology* **352**:585–596 DOI 10.1016/j.jmb.2005.07.013.

Blanc G, Wolfe KH. 2004. Widespread paleopolyploidy in model plant species inferred from age distributions of duplicate genes. *The Plant Cell* **16**:1667–1678 DOI 10.1105/tpc.021345.

Cardon G, Hohmann S, Klein J, Nettesheim K, Saedler H, Huijser P. 1999. Molecular characterisation of the Arabidopsis *SBP-box* genes. *Gene* **237**:91–104 DOI 10.1016/s0378-1119(99)00308-x.

Chao LM, Liu YQ, Chen DY, Xue XY, Mao YB, Chen XY. 2017. Arabidopsis transcription factors SPL1 and SPL12 confer plant thermotolerance at reproductive stage. *Molecular Plant* **10**:735–748 DOI 10.1016/j.molp.2017.03.010.

Chen C, Chen H, Zhang Y, Thomas HR, Frank MH, He Y, Xia R. 2020. TBtools: an integrative toolkit developed for interactive analyses of big biological data. *Molecular Plant* **13**:1194–1202 DOI 10.1016/j.molp.2020.06.009.

Chen G, Li J, Liu Y, Zhang Q, Gao Y, Fang K, Cao Q, Qin L, Xing Y. 2019. Roles of the GA-mediated *SPL* gene family and *miR156* in the floral development of Chinese Chestnut (*Castanea mollissima*). *International Journal of Molecular Sciences* **20**:1577 DOI 10.3390/ijms20071577.

Cheng H, Hao M, Wang W, Mei D, Tong C, Wang H, Liu J, Fu L, Hu Q. 2016. Genomic identification, characterization and differential expression analysis of *SBP-box* gene family in *Brassica napus*. *BMC Plant Biology* **16**:196 DOI 10.1186/s12870-016-0852-y.

Colebrook EH, Thomas SG, Phillips AL, Hedden P. 2014. The role of gibberellin signalling in plant responses to abiotic stress. *Journal of Experimental Biology* **217**:67–75 DOI 10.1242/jeb.089938.

Cui L, Zheng F, Wang J, Zhang C, Xiao F, Ye J, Li C, Ye Z, Zhang J. 2020. miR156a-targeted SBP-Box transcription factor SlSPL13 regulates inflorescence morphogenesis by directly activating *SFT* in tomato. *Plant Biotechnology Journal* **18**:1670–1682 DOI 10.1111/pbi.13331.

Dai X, Zhuang Z, Zhao PX. 2018. psRNATarget: a plant small RNA target analysis server (2017 release). *Nucleic Acids Research* **46**:W49–W54 DOI 10.1093/nar/gky316.

Dong X. 1998. SA, JA, ethylene, and disease resistance in plants. *Current Opinion in Plant Biology* **1**:316–323 DOI 10.1016/1369-5266(88)80053-0.

El-Gebali S, Mistry J, Bateman A, Eddy SR, Luciani A, Potter SC, Qureshi M, Richardson LJ, Salazar GA, Smart A, Sonnhammer ELL, Hirsh L, Paladin L, Piovesan D, Tosatto SCE, Finn RD. 2019. The Pfam protein families database in 2019. *Nucleic Acids Research* **47**:D427–D432 DOI 10.1093/nar/gky995.

Feng X, Wang Y, Zhang N, Zhang X, Wu J, Huang Y, Ruan M, Zhang J, Qi Y. 2021. Systematic identification, evolution and expression analysis of the *SPL* gene family in Sugarcane (*Saccharum spontaneum*). *Tropical Plant Biology* **14**:313–328 DOI 10.1007/s12042-021-09293-4.

Ferreirae Silva GF, Silva EM, Azevedo M da S, Guivin MA, Ramiro DA, Figueiredo CR, Carrer H, Peres LE, Nogueira FT. 2014. microRNA156-targeted SPL/SBP box transcription factors regulate tomato ovary and fruit development. *The Plant Journal* **78**:604–618 DOI 10.1111/tpj.12493.

Finn RD, Bateman A, Clements J, Coggill P, Eberhardt RY, Eddy SR, Heger A, Hetherington K, Holm L, Mistry J, Sonnhammer EL, Tate J, Punta M. 2014. Pfam: the protein families database. *Nucleic Acids Research* **42**:D222–D230 DOI 10.1093/nar/gkt1223.

Gandikota M, Birkenbihl RP, Hohmann S, Cardon GH, Saedler H, Huijser P. 2007. The *miRNA156/157* recognition element in the 3′ UTR of the Arabidopsis *SBP box* gene *SPL3* prevents early flowering by translational inhibition in seedlings. *The Plant Journal* **49**:683–693 DOI 10.1111/j.1365-313X.2006.02983.x.

Glazebrook J. 2005. Contrasting mechanisms of defense against biotrophic and necrotrophic pathogens. *Annual Review of Phytopathology* **43**:205–227 DOI 10.1146/annurev.phyto.43.040204.135923.

Guo AY, Zhu QH, Gu X, Ge S, Yang J, Luo J. 2008. Genome-wide identification and evolutionary analysis of the plant specific SBP-box transcription factor family. *Gene* **418**:1–8 DOI 10.1016/j.gene.2008.03.016.

Hoang TV, Vo KTX, Rahman MM, Choi SH, Jeon JS. 2019. Heat stress transcription factor OsSPL7 plays a critical role in reactive oxygen species balance and stress responses in rice. *Plant Science* **289**:110273 DOI 10.1016/j.plantsci.2019.110273.

Hou H, Jia H, Yan Q, Wang X. 2018. Overexpression of a *SBP-box* gene (*VpSBP16*) from Chinese Wild Vitis Species in *Arabidopsis* improves salinity and drought stress tolerance. *International Journal of Molecular Sciences* **19**:940 DOI 10.3390/ijms19040940.

Hou H, Li J, Gao M, Singer SD, Wang H, Mao L, Fei Z, Wang X. 2013. Genomic organization, phylogenetic comparison and differential expression of the *SBP-box* family genes in grape. *PLOS ONE* **8**:e59358 DOI 10.1371/journal.pone.0059358.

Jerome Jeyakumar JM, Ali A, Wang WM, Thiruvengadam M. 2020. Characterizing the role of the *miR156-SPL* network in plant development and stress response. *Plants* **9**:1026 DOI 10.3390/plants9091206.

Jung JH, Ju Y, Seo PJ, Lee JH, Park CM. 2012. The *SOC1-SPL* module integrates photoperiod and gibberellic acid signals to control flowering time in *Arabidopsis*. *The Plant Journal* **69**:577–588 DOI 10.1111/j.1365-313X.2011.04813.x.

Kastoori Ramamurthy R, Xiang Q, Hsieh EJ, Liu K, Zhang C, Waters BM. 2018. New aspects of iron-copper crosstalk uncovered by transcriptomic characterization of Col-0 and the copper uptake mutant *spl7* in *Arabidopsis thaliana*. *Metallomics* **10**:1824–1840 DOI 10.1039/c8mt00287h.

Kim Y, Mun BG, Khan AL, Waqas M, Kim HH, Shahzad R, Imran M, Yun BW, Lee IJ. 2018. Regulation of reactive oxygen and nitrogen species by salicylic acid in rice plants under salinity stress conditions. *PLOS ONE* **13**:e0192650 DOI 10.1371/journal.pone.0192650.

Klein J, Saedler H, Huijser P. 1996. A new family of DNA binding proteins includes putative transcriptional regulators of the *Antirrhinum majus* floral meristem identity gene *SQUAMOSA*. *Molecular and General Genetics* **250**:7–16 DOI 10.1007/BF02191820.

Kropat J, Tottey S, Birkenbihl RP, Depege N, Huijser P, Merchant S. 2005. A regulator of nutritional copper signaling in *Chlamydomonas* is an SBP domain protein that recognizes the GTAC core of copper response element. *Proceedings of the National Academy of Sciences of the United States of America* **102**:18730–18735 DOI 10.1073/pnas.0507693102.

Kumar S, Stecher G, Tamura K. 2016. MEGA7: molecular evolutionary genetics analysis version 7.0 for bigger datasets. *Molecular Biology and Evolution* **33**:1870–1874 DOI 10.1093/molbev/msw054.

Lan T, Zheng Y, Su Z, Yu S, Song H, Zheng X, Lin G, Wu W. 2019. OsSPL10, a *SBP-Box* gene, plays a dual role in salt tolerance and trichome formation in rice (*Oryza sativa L.*). *G3* **9**:4107–4114 DOI 10.1534/g3.119.400700.

Lee H, Noh H, Mun J, Gu C, Sever S, Park S. 2016. Anks1a regulates COPII-mediated anterograde transport of receptor tyrosine kinases critical for tumorigenesis. *Nature Communications* **7**:12799 DOI 10.1038/ncomms12799.

Lescot M, Dehais P, Thijs G, Marchal K, Moreau Y, VandePeer Y, Rouze P, Rombauts S. 2002. PlantCARE, a database of plant cis-acting regulatory elements and a portal to tools for in silico analysis of promoter sequences. *Nucleic Acids Research* **30**:325–327 DOI 10.1093/nar/30.1.325.

Li B, Zhao Y, Wang S, Zhang X, Wang Y, Shen Y, Yuan Z. 2021. Genome-wide identification, gene cloning, subcellular location and expression analysis of *SPL* gene family in *P. granatum* L. *BMC Plant Biology* **21**:400 DOI 10.1186/s12870-021-03171-7.

Li J, Hou H, Li X, Xiang J, Yin X, Gao H, Zheng Y, Bassett CL, Wang X. 2013. Genome-wide identification and analysis of the *SBP-box* family genes in apple (*Malus x domestica Borkh.*). *Plant Physiology and Biochemistry* **70**:100–114 DOI 10.1016/j.plaphy.2013.05.021.

Li Y, Song Q, Zhang Y, Li Z, Guo J, Chen X, Zhang G. 2020. Genome-wide identification, characterization, and expression patterns analysis of the *SBP-box* gene family in wheat (*Triticum aestivum* L.). *Scientific Reports* **10**:17250 DOI 10.1038/s41598-020-74417-x.

Librado P, Rozas J. 2009. DnaSP v5: a software for comprehensive analysis of DNA polymorphism data. *Bioinformatics* **25**:1451–1452 DOI 10.1093/bioinformatics/btp187.

Liu J, Cheng X, Liu P, Sun J. 2017a. miR156-Targeted SBP-Box transcription factors interact with DWARF53 to regulate *TEOSINTE BRANCHED1* and *BARREN STALK1* expression in bread wheat. *Plant Physiology* **174**:1931–1948 DOI 10.1104/pp.17.00445.

Liu N, Tu L, Wang L, Hu H, Xu J, Zhang X. 2017b. MicroRNA157-targeted *SPL* genes regulate floral organ size and ovule production in cotton. *BMC Plant Biology* **17**:7 DOI 10.1186/s12870-016-0969-z.

Liu X, Xia B, Purente N, Chen B, Zhou Y, He M. 2021a. Transgenic *Chrysanthemum indicum* overexpressing *cin-miR396a* exhibits altered plant development and reduced salt and drought tolerance. *Plant Physiology and Biochemistry* **168**:17–26 DOI 10.1016/j.plaphy.2021.09.035.

Liu Y, Aslam M, Yao LA, Zhang M, Wang L, Chen H, Huang Y, Qin Y, Niu X. 2021b. Genomic analysis of *SBP* gene family in *Saccharum spontaneum* reveals their association with vegetative and reproductive development. *BMC Genomics* **22**:767 DOI 10.1186/s12864-021-08090-3.

Ma Y, Xue H, Zhang F, Jiang Q, Yang S, Yue P, Wang F, Zhang Y, Li L, He P, Zhang Z. 2021. The *miR156/SPL* module regulates apple salt stress tolerance by activating *MdWRKY100* expression. *Plant Biotechnology Journal* **19**:311–323 DOI 10.1111/pbi.13464.

Ma YP, Zhao L, Zhang WJ, Zhang YH, Xing X, Duan XX, Hu J, Harris A, Liu PL, Dai SL, Wen J. 2020. Origins of cultivars of Chrysanthemum—Evidence from the chloroplast genome and nuclear *LFY* gene. *Journal of Systematics and Evolution* **58**:925–944 DOI 10.1111/jse.12682.

Mittler R, Blumwald E. 2015. The roles of ROS and ABA in systemic acquired acclimation. *The Plant Cell* **27**:64–70 DOI 10.1105/tpc.114.133090.

Mulder N, Apweiler R. 2007. InterPro and InterProScan: tools for protein sequence classification and comparison. *Methods in Molecular Biology* **396**:59–70 DOI 10.1007/978-1-59745-515-2_5.

Pan F, Wang Y, Liu H, Wu M, Chu W, Chen D, Xiang Y. 2017. Genome-wide identification and expression analysis of SBP-like transcription factor genes in Moso Bamboo (*Phyllostachys edulis*). *BMC Genomics* **18**:486 DOI 10.1186/s12864-017-3882-4.

Peng X, Wang Q, Zhao Y, Li X, Ma Q. 2019. Comparative genome analysis of the *SPL* gene family reveals novel evolutionary features in maize. *Genetics and Molecular Biology* **42**:380–394 DOI 10.1590/1678-4685-GMB-2017-0144.

Pfaffl MW. 2001. A new mathematical model for relative quantification in real-time RT-PCR. *Nucleic Acids Research* **29**:e45 DOI 10.1093/nar/29.9.e45.

Preston JC, Jorgensen SA, Orozco R, Hileman LC. 2016. Paralogous *SQUAMOSA PROMOTER BINDING PROTEIN-LIKE* (*SPL*) genes differentially regulate leaf initiation and reproductive phase change in petunia. *Planta* **243**:429–440 DOI 10.1007/s00425-015-2413-2.

Qi S, Twyford AD, Ding JY, Borrell JS, Wang LZ, Ma YP, Wang N. 2021. Natural interploidy hybridization among the key taxa involved in the origin of horticultural chrysanthemums. *Journal of Systematics and Evolution* **00**:1–10 DOI 10.1111/jse.12810.

Qiu Z, Guo J, Zhu A, Zhang L, Zhang M. 2014. Exogenous jasmonic acid can enhance tolerance of wheat seedlings to salt stress. *Ecotoxicology and Environmental Safety* **104**:202–208 DOI 10.1016/j.ecoenv.2014.03.014.

Ren L, Sun J, Chen S, Gao J, Dong B, Liu Y, Xia X, Wang Y, Liao Y, Teng N, Fang W, Guan Z, Chen F, Jiang J. 2014. A transcriptomic analysis of *Chrysanthemum nankingense* provides insights into the basis of low temperature tolerance. *BMC Genomics* **15**:844 DOI 10.1186/1471-2164-15-844.

Riese M, Hohmann S, Saedler H, Munster T, Huijser P. 2007. Comparative analysis of the *SBP-box* gene families in *P. patens* and seed plants. *Gene* **401**:28–37 DOI 10.1016/j.gene.2007.06.018.

Sah SK, Reddy KR, Li J. 2016. Abscisic acid and abiotic stress tolerance in crop plants. *Frontiers in Plant Science* **7**:571 DOI 10.3389/fpls.2016.00571.

Saibo NJ, Lourenco T, Oliveira MM. 2009. Transcription factors and regulation of photosynthetic and related metabolism under environmental stresses. *Annals of Botany* **103**:609–623 DOI 10.1093/aob/mcn227.

Schwarz S, Grande AV, Bujdoso N, Saedler H, Huijser P. 2008. The microRNA regulated *SBP-box* genes *SPL9* and *SPL15* control shoot maturation in *Arabidopsis*. *Plant Molecular Biology* **67**:183–195 DOI 10.1007/s11103-008-9310-z.

Shao Y, Zhou HZ, Wu Y, Zhang H, Lin J, Jiang X, He Q, Zhu J, Li Y, Yu H, Mao C. 2019. OsSPL3, an SBP-Domain protein, regulates crown root development in rice. *The Plant Cell* **31**:1257–1275 DOI 10.1105/tpc.19.00038.

Skirycz A, Inze D. 2010. More from less: plant growth under limited water. *Current Opinion in Biotechnology* **21**:197–203 DOI 10.1016/j.copbio.2010.03.002.

Song C, Liu Y, Song A, Dong G, Zhao H, Sun W, Ramakrishnan S, Wang Y, Wang S, Li T, Niu Y, Jiang J, Dong B, Xia Y, Chen S, Hu Z, Chen F, Chen S. 2018. The *Chrysanthemum nankingense* genome provides insights into the evolution and diversification of chrysanthemum flowers and medicinal traits. *Molecular Plant* **11**:1482–1491 DOI 10.1016/j.molp.2018.10.003.

Song M, Wang H, Ma H, Zheng C. 2022. Genome-wide analysis of *JAZ* family genes expression patterns during fig (*Ficus carica* L.) fruit development and in response to hormone treatment. *BMC Genomics* **23**:170 DOI 10.1186/s12864-022-08420-z.

Song N, Cheng Y, Peng W, Peng E, Zhao Z, Liu T, Yi T, Dai L, Wang B, Hong Y. 2021. Genome-wide characterization and expression analysis of the *SBP-Box* gene family in sweet orange (*Citrus sinensis*). *International Journal of Molecular Sciences* **22**:8918 DOI 10.3390/ijms22168918.

Song A, Gao T, Wu D, Xin J, Chen S, Guan Z, Wang H, Jin L, Chen F. 2016. Transcriptome-wide identification and expression analysis of chrysanthemum SBP-like transcription factors. *Plant Physiology and Biochemistry* **102**:10–16 DOI 10.1016/j.plaphy.2016.02.009.

Stief A, Altmann S, Hoffmann K, Pant BD, Scheible WR, Baurle I. 2014. Arabidopsis *miR156* regulates tolerance to recurring environmental stress through SPL transcription factors. *The Plant Cell* **26**:1792–1807 DOI 10.1105/tpc.114.123851.

Stone JM, Liang X, Nekl ER, Stiers JJ. 2005. Arabidopsis AtSPL14, a plant-specific SBP-domain transcription factor, participates in plant development and sensitivity to fumonisin B1. *The Plant Journal* **41**:744–754 DOI 10.1111/j.1365-313X.2005.02334.x.

Tang M, Zhou C, Meng L, Mao D, Peng C, Zhu Y, Huang D, Tan Z, Chen C, Liu C, Zhang D. 2016. Overexpression of *OsSPL9* enhances accumulation of Cu in rice grain and improves its digestibility and metabolism. *Journal of Genetics and Genomics* **43**:673–676 DOI 10.1016/j.jgg.2016.09.004.

Teng RM, Wang YX, Li H, Liu H, Wang Y, Zhuang J. 2021. Identification and expression analysis of the *SBP-box* gene family related to abiotic stress in tea plant (*Camellia sinensis* (L.) O. Kuntze). *Plant Molecular Biology Reporter* **40**:148–162 DOI 10.1007/s11105-021-01306-6.

Tregear JW, Richaud F, Collin M, Esbelin J, Parrinello H, Cochard B, Nodichao L, Morcillo F, Adam H, Jouannic S. 2022. Micro-RNA-Regulated *SQUAMOSA-PROMOTER BINDING PROTEIN-LIKE* (*SPL*) gene expression and cytokinin accumulation distinguish early-developing male and female inflorescences in Oil Palm (*Elaeis guineensis*). *Plants* **11**:685 DOI 10.3390/plants11050685.

Unte US, Sorensen AM, Pesaresi P, Gandikota M, Leister D, Saedler H, Huijser P. 2003. SPL8, an *SBP-box* gene that affects pollen sac development in *Arabidopsis*. *The Plant Cell* **15**:1009–1019 DOI 10.1105/tpc.010678.

Wang J, Ye Y, Xu M, Feng L, Xu LA. 2019. Roles of the *SPL* gene family and *miR156* in the salt stress responses of tamarisk (*Tamarix chinensis*). *BMC Plant Biology* **19**:370 DOI 10.1186/s12870-019-1977-6.

Wang M, Mo Z, Lin R, Zhu C. 2021. Characterization and expression analysis of the *SPL* gene family during floral development and abiotic stress in pecan (*Carya illinoinensis*). *PeerJ* **9**:e12490 DOI 10.7717/peerj.12490.

Wang S, Wu K, Yuan Q, Liu X, Liu Z, Lin X, Zeng R, Zhu H, Dong G, Qian Q, Zhang G, Fu X. 2012. Control of grain size, shape and quality by *OsSPL16* in rice. *Nature Genetics* **44**:950–954 DOI 10.1038/ng.2327.

Wang Y, Hu Z, Yang Y, Chen X, Chen G. 2009. Function annotation of an *SBP-box* gene in *Arabidopsis* based on analysis of co-expression networks and promoters. *International Journal of Molecular Sciences* **10**:116–132 DOI 10.3390/ijms10010116.

Wang Y, Zhou LJ, Wang Y, Geng Z, Liu S, Chen C, Chen S, Jiang J, Chen F. 2022. CmMYB9a activates floral coloration by positively regulating anthocyanin biosynthesis in chrysanthemum. *Plant Molecular Biology* **108**:51–63 DOI 10.1007/s11103-021-01206-z.

Won SY, Kwon SJ, Lee TH, Jung JA, Kim JS, Kang SH, Sohn SH. 2017. Comparative transcriptome analysis reveals whole-genome duplications and gene selection patterns in cultivated and wild Chrysanthemum species. *Plant Molecular Biology* **95**:451–461 DOI 10.1007/s11103-017-0663-z.

Xie K, Wu C, Xiong L. 2006. Genomic organization, differential expression, and interaction of *SQUAMOSA* promoter-binding-like transcription factors and *microRNA156* in rice. *Plant Physiology* **142**:280–293 DOI 10.1104/pp.106.084475.

Xing S, Salinas M, Hohmann S, Berndtgen R, Huijser P. 2010. miR156-targeted and nontargeted SBP-box transcription factors act in concert to secure male fertility in *Arabidopsis*. *The Plant Cell* **22**:3935–3950 DOI 10.1105/tpc.110.079343.

Xu M, Hu T, Zhao J, Park MY, Earley KW, Wu G, Yang L, Poethig RS. 2016. Developmental functions of *miR156*-Regulated *SQUAMOSA PROMOTER BINDING PROTEIN-LIKE* (*SPL*) genes in *Arabidopsis thaliana*. *PLOS Genetics* **12**:e1006263 DOI 10.1371/journal.pgen.1006263.

Yamaguchi A, Wu MF, Yang L, Wu G, Poethig RS, Wagner D. 2009. The *microRNA*-regulated SBP-Box transcription factor SPL3 is a direct upstream activator of *LEAFY, FRUITFULL*, and *APETALA1*. *Developmental Cell* **17**:268–278 DOI 10.1016/j.devcel.2009.06.007.

Yamasaki H, Hayashi M, Fukazawa M, Kobayashi Y, Shikanai T. 2009. SQUAMOSA promoter binding protein-Like7 is a central regulator for copper homeostasis in arabidopsis. *The Plant Cell* **21**:347–361 DOI 10.1105/tpc.108.060137.

Yamasaki K, Kigawa T, Inoue M, Tateno M, Yamasaki T, Yabuki T, Aoki M, Seki E, Matsuda T, Nunokawa E, Ishizuka Y, Terada T, Shirouzu M, Osanai T, Tanaka A, Seki M, Shinozaki K, Yokoyama S. 2004. A novel zinc-binding motif revealed by solution structures of DNA-binding domains of *Arabidopsis* SBP-family transcription factors. *Journal of Molecular Biology* **337**:49–63 DOI 10.1016/j.jmb.2004.01.015.

Yang W, Glover BJ, Rao GY, Yang J. 2006. Molecular evidence for multiple polyploidization and lineage recombination in the *Chrysanthemum indicum* polyploid complex (*Asteraceae*). *New Phytologist* **171**:875–886 DOI 10.1111/j.1469-8137.2006.01779.x.

Yang X, Wang J, Dai Z, Zhao X, Miao X, Shi Z. 2019. miR156f integrates panicle architecture through genetic modulation of branch number and pedicel length pathways. *Rice* **12**:40 DOI 10.1186/s12284-019-0299-5.

Yang Z, Wang X, Gu S, Hu Z, Xu H, Xu C. 2008. Comparative study of *SBP-box* gene family in *Arabidopsis* and rice. *Gene* **407**:1–11 DOI 10.1016/j.gene.2007.02.034.

Yuan H, Qin P, Hu L, Zhan S, Wang S, Gao P, Li J, Jin M, Xu Z, Gao Q, Du A, Tu B, Chen W, Ma B, Wang Y, Li S. 2019. OsSPL18 controls grain weight and grain number in rice. *Journal of Genetics and Genomics* **46**:41–51 DOI 10.1016/j.jgg.2019.01.003.

Zhang D, Han Z, Li J, Qin H, Zhou L, Wang Y, Zhu X, Ma Y, Fang W. 2020. Genome-wide analysis of the *SBP-box* gene family transcription factors and their responses to abiotic stresses in tea (*Camellia sinensis*). *Genomics* **112**:2194–2202 DOI 10.1016/j.ygeno.2019.12.015.

Zhang X, Dou L, Pang C, Song M, Wei H, Fan S, Wang C, Yu S. 2015. Genomic organization, differential expression, and functional analysis of the *SPL* gene family in *Gossypium hirsutum*. *Molecular Genetics and Genomics* **290**:115–126 DOI 10.1007/s00438-014-0901-x.

Zhang X, Zhang F, Zhao H, Guan Z, Chen S, Jiang J, Fang W, Chen F. 2014. Comparative analysis of genetic diversity among species of Chrysanthemum and its related genera using inter-simple sequence repeat and sequence-related amplified polymorphism markers. *Genetics and Molecular Research* **13**:8469–8479 DOI 10.4238/2014.October.20.23.

Zhu L, Guan Y, Liu Y, Zhang Z, Jaffar MA, Song A, Chen S, Jiang J, Chen F. 2020. Regulation of flowering time in chrysanthemum by the R2R3 MYB transcription factor CmMYB2 is associated with changes in gibberellin metabolism. *Horticulture Research* **7**:96 DOI 10.1038/s41438-020-0317-1.